

3-HYDROXY-3-METHYLGLUTARYL-COENZYME A LYASE:  
INVESTIGATION OF CYSTEINES MEDIATING INTERSUBUNIT DISULFIDE  
FORMATION AND REGULATION BY THIOL-DISULFIDE EXCHANGE  
AND  
DISCOVERY OF AN EXTRAMITOCHONDRIAL HOMOLOG

A DISSERTATION IN  
Molecular Biology and Biochemistry  
and  
Cell Biology and Biophysics

Presented to the Faculty of the University  
of Missouri-Kansas City in partial fulfillment of  
the requirements for the degree

DOCTOR OF PHILOSOPHY

by  
CHRISTA L. COCHRAN MONTGOMERY

M.S., University of Missouri-Kansas City, 2004  
B.S., University of Missouri-Kansas City, 1995

Kansas City, MO  
2011



3-HYDROXY-3-METHYLGLUTARYL-COENZYME A LYASE:  
INVESTIGATION OF CYSTEINES MEDIATING INTERSUBUNIT DISULFIDE  
FORMATION AND REGULATION BY THIOL-DISULFIDE EXCHANGE  
AND  
DISCOVERY OF AN EXTRAMITOCHONDRIAL HOMOLOG

Christa L. Cochran Montgomery, Candidate for the Doctor of Philosophy Degree  
University of Missouri-Kansas City, 2011

ABSTRACT

3-Hydroxy-3-methylglutaryl-Coenzyme A lyase catalyzes the cleavage of 3-hydroxy-3-methylglutaryl-Coenzyme A into acetoacetate and acetyl-Coenzyme A, a key reaction in ketogenesis and leucine catabolism. Previous work prompted the hypothesis that in the absence of reductant, cysteine 323 forms a disulfide bond with cysteine 323 on the adjacent monomer, blocking the substrate's access to the active site which results in diminished enzyme activity. The recently published crystal structure of the human enzyme indicates that cysteines 323 on each monomer are too far apart to form a disulfide. Each of the eight cysteines has been individually mutated to serine and the mutants analyzed for activity and dimer formation in the presence and absence of reductant. C170S, C266S, and C323S do not form dimers in the absence of reductant. C170S, C197S, and C234S have an inflated dependence on thiol, C174S, C307S, and

C323S a near wild-type dependence, and C141S and C266S a reduced dependence. Therefore intersubunit disulfide bond formation does not directly correlate with diminution of activity in the absence of thiol as previously proposed. Analysis of C170S/C174S, C170S/C266S and C170S/C323S double mutants demonstrate that C170S is not directly involved in the intersubunit disulfide bond and suggest that C170 may be involved in regulation of activity by thiol/disulfide exchange. A C266S/C323S mutant heterodimer restores covalent dimer formation confirming that these residues are involved in intersubunit disulfide bond formation. Based on sequence homology, the Mammalian Gene Collection Program identified the protein encoded by the gene 3-hydroxy-3-methylglutaryl-Coenzyme A lyase-like 1 as being a potential 3-hydroxy-3-methylglutaryl-Coenzyme A lyase. Characterization of the purified recombinant human protein confirms that it is an authentic 3-hydroxy-3-methylglutaryl-Coenzyme A lyase. In-vitro myristoylation experiments confirm that the protein is modified by N-myristoyltransferase and immunofluorescence microscopy in COSI cells demonstrate that this modification effects the subcellular localization of the protein. Blots of rodent organ lysates reveal expression primarily in the small intestine and that the protein is overexpressed in human neuroblastoma and glioma cell lines compared to mouse brain. Co-localization experiments failed to determine to which compartment the lyase-like protein is localized but confirm it is not mitochondrial or peroxisomal as is the traditional lyase.

The faculty listed below, appointed by the Dean of the School of Graduate Studies, have examined a dissertation titled “*3-Hydroxy-3-methylglutaryl-Coenzyme A Lyase: Investigation of Cysteines Mediating Intersubunit Disulfide Formation and Regulation by Thiol/Disulfide Exchange AND Discovery of an Extramitochondrial Homolog*” presented by Christa L. Cochran Montgomery, candidate for the Doctor of Philosophy degree, and certify that in their opinion it is worthy of acceptance.

Supervisory Committee

Henry M. Miziorko, Ph.D., Committee Chair  
Division of Molecular Biology and Biochemistry

Karen Bame, Ph.D.  
Division of Molecular Biology and Biochemistry

Brian Geisbrecht, Ph.D.  
Division of Cell Biology and Biophysics

Anthony Persechini, Ph.D.  
Division of Molecular Biology and Biochemistry

Marilyn Yoder, Ph.D.  
Division of Cell Biology and Biophysics

## CONTENTS

ABSTRACT.....	iii
ILLUSTRATIONS.....	x
TABLES.....	xii
ABBREVIATIONS.....	xiii
ACKNOWLEDGMENTS.....	xix
CHAPTER	
1. INTRODUCTION.....	1
Ketogenesis.....	1
Regulation of Ketogenesis.....	2
3-Hydroxy-3-methylglutaryl-Coenzyme A Lyase.....	4
HMG-CoA Lyase Deficiency.....	7
2. INFLUENCE OF MULTIPLE CYSTEINES ON HUMAN HMG-COA LYASE ACTIVITY AND FORMATION OF INTERSUBUNIT ADDUCTS.....	8
Introduction.....	8
Materials and Methods.....	9
Materials.....	9
Plasmid Construction.....	10
Protein Expression.....	10
Mutagenesis.....	11
Enzyme Purification.....	12
Enzyme Activity Measurement.....	13

Preparation of Nonreduced Enzyme.....	13
NEM Modification.....	14
SDS-PAGE and Western Blotting.....	14
Results.....	15
Location of Cysteine Residues in Native Human HMGCL.....	15
Reduction of Microheterogeneity in SDS PAGE Mobility Upon N-Ethylmaleimide Modification of Nonreduced HMGCL.....	18
Strategy for Evaluation of Cysteine Residue Contributions to Disulfide Bond Formation and to Enzyme Activity in the Presence or Absence of Reductant.....	19
Influence of Cysteine Substitutions on Intersubunit Adduct Formation in Nonreduced Protein.....	22
Coexpression of HMGCL C266S and C323S Proteins Supports Formation of a Heterodimer that Forms a Covalent Intersubunit Adduct.....	24
Influence of Individual Cysteines on HMGCL Catalytic Activity.....	26
Investigation of the Possible Interaction Between Cysteines C170 and C174 as an Influence on Formation of Intersubunit Dimer Adducts.....	29
Discussion.....	32
Magnitude of Dependence on Exogenous Reductants does not Correlate with Formation of Intersubunit Adducts.....	32
Competition for C266 may Reflect Participation of Several HMGCL Cysteines in Formation of Disulfide Bonds.....	33
3. DISCOVERY OF AN EXTRAMITOCHONDRIAL HUMAN HMG-COA LYASE.....	37
Introduction.....	37
Materials and Methods.....	38

Materials.....	38
Plasmid Construction.....	39
Mutagenesis.....	40
Expression of HMGCLL1 in Inclusion Bodies.....	40
Purification of HMGCLL1 from Inclusion Bodies.....	41
Antibody Production and Purification.....	42
Native Protein Expression.....	43
Native Enzyme Purification.....	44
Enzyme Activity Measurement.....	45
Expression and Purification of Human N-myristoyltransferase.....	46
In-vitro N-myristoylation Assay.....	47
Immunofluorescence in COSI Cells.....	47
Rat Organ Lysate Blots.....	48
Immunofluorescence in Neuro2a and U87 Cells.....	49
Results.....	50
Comparison of Human HMGCL and Human HMGCLL1 Amino Acid Sequences.....	50
Specificity of Anti-HMGCLL1 Antibody.....	52
Expression and Purification of HMGCLL1.....	54
Functional Characterization of HMGCLL1.....	58
In-vitro Myristoylation of HMGCLL1.....	60
Localization of HMGCLL1 in COS1 cells.....	62
Endogenous Expression of HMGCLL1 in Rat Organ Lysates.....	65

Endogenous Expression in Mouse and Human Neuroblastoma and Human Glioblastoma Cell Lines.....	67
Indirect Immunofluorescence of HMGCLL1 in Neuro2a and U87 Cells.....	70
Discussion.....	72
4. CONCLUSIONS AND FUTURE DIRECTIONS.....	76
Investigation of Cysteines Mediating Intersubunit Disulfide Formation and Regulation by Thiol-Disulfide Exchange.....	76
Discovery of an Extramitochondrial Homolog of HMG-CoA Lyase.....	78
REFERENCE LIST.....	81
VITA.....	90

## ILLUSTRATIONS

Figure	Page
1.1 Structures of the ketone bodies.....	1
1.2 The enzymatic steps of ketogenesis.....	3
2.1 Crystal structure of HMGCL and distances between cysteine sulfurs.....	16
2.2 Sequence alignment of diverse eukaryotic and prokaryotic HMG-CoA lyase proteins.....	18
2.3 SDS-PAGE of human HMGCL under reducing or nonreducing conditions.....	20
2.4 Western blots of human HMGCL Cys → Ser mutants under reducing [A] or nonreducing [B] conditions.....	23
2.5 Western blot of human HMGCL and pET30HL C266S / pTrcHL C323S heterodimer under reducing and nonreducing conditions.....	25
2.6 Western blots of human HMGCL C170S double mutants under reducing [A] or nonreducing [B] conditions.....	31
2.7 Basic model for residues competing in disulfide bond formation.....	35
3.1 A sequence alignment comparing the sequences of HMG-CoA lyase and HMGCLL1 from <i>Homo sapiens</i> (human).....	51
3.2 A sequence alignment comparing the N-terminal sequences of human HMG-CoA lyase and HMNGCLL1 from a variety of vertebrates.....	53
3.3 Specificity of anti-HMGCLL1 antibody.....	55
3.4 The anti-HMGCLL1 antibody does not react with endogenous <i>E. coli</i> or <i>P. pastoris</i> proteins.....	56
3.5 SDS gels (A, C) and Western blots (B, D) of fractions from the purification of wild-type (A, B) and G2A (C, D) HMGCLL1.....	57
3.6 Coomassie stained Western blot of wt (lanes 1-3 and 7-9) and G2A HMGCLL1 (lanes 4-6) produced in <i>E. coli</i> (lanes 1-3) and <i>P. pastoris</i> (lanes 4-9).....	59

3.7	Autoradiograph demonstrating <i>in-vitro</i> myristoylation of HMGCLL1.....	63
3.8	Immunofluorescence microscopy of COS-1 cells overexpressing HMGCLL1 or G2A HMGCLL1.....	64
3.9	Rat organ lysate blots probed with anti-HMGCL (A) or anti-HMGCLL1 (B) antibodies.....	66
3.10	Western blot of mouse organ and human cancer cell line homogenates.....	68
3.11	Western blot of neuro2a supernatant probed with anti-HMGCLL1 antibody.....	69
3.12	Indirect immunofluorescence of HMGCLL1 in neuro2a (A) and U87 cells (B)..	71
3.13	Subcellular localization of HMGCLL1 in neuro2a cells.....	73

## TABLES

Table	Page
1.1 Effects of insulin and glucagon on key enzymes controlling ketogenesis.....	5
1.2 Characteristics of HMG-CoA lyases.....	6
2.1 Dependence of activity of human HMGCL single Cys → Ser mutants on exogenous thiol.....	28
2.2 Dependence of activity of HMGCL double Cys → Ser mutants on exogenous thiol.....	30
3.1 Characterization of Human Wild-type and G2A HMGCLL1.....	60
3.2 Edman Degradation <sup>a</sup> of Wild-type and G2A HMGCLL1.....	61

## ABBREVIATIONS

A <sub>340</sub>	absorbance at 340 nanometers
A <sub>280</sub>	absorbance at 280 nanometers
AcAc	acetoacetic acid
ATP	adenosine 5'-triphosphate
A	alanine
Amp	ampicillin
Å	angstrom
R	arginine
<i>Bam</i>	<i>Bacillus amyloliquefaciens</i>
<i>B. subtilis</i>	<i>Bacillus subtilis</i>
BODIPY	boron-dipyrromethene
BSA	bovine serum albumin
CO <sub>2</sub>	carbon dioxide
C-terminal	carboxy-terminal
CPTI	carnitine palmitoyl transferase 1
COS1	cell line from African green monkey kidney
Cl	chloride
CoA	coenzyme A
Cy3	cyanine dye 3
C or Cys	cysteine

°C	degrees celsius
DNA	deoxyribonucleic acid
dNTP	Deoxyribonucleotide triphosphate
2D	2-dimensional
<i>D. pneumoniae</i>	<i>Diplococcus pneumoniae</i>
DTT	dithiothreitol
<i>D. melanogaster</i>	<i>Drosophila melanogaster</i>
D-PBS	Dulbecco's phosphate-buffered saline
ECL	<i>enhanced chemiluminescence</i>
<i>E. coli</i>	<i>Escherichia coli</i>
EGTA	ethylene glycol tetraacetic acid
EDTA	ethylenediaminetetraacetic acid
$\epsilon$	extinction coefficient
for	forward
<i>G. gallus</i>	<i>Gallus gallus</i>
GE	<i>general electric</i>
Q	glutamine
G	glycine
GdHCl	guanidine hydrochloride
H or His	histidine
<i>H. sapiens</i>	<i>Homo sapiens</i>
HSL	hormone sensitive lipase

hr(s)	hour(s)
HMG-CoA	3-hydroxy-3-methylglutaryl-Coenzyme A
HMG-CoA lyase, HMGCL, or HL	3-hydroxy-3-methylglutaryl-Coenzyme A Lyase
HMGCLL1	3-hydroxy-3-methylglutaryl-Coenzyme A lyase-like 1
3HBDH	3-hydroxybutyrate dehydrogenase
3HB	3-hydroxybutyric acid
HEPES	4-(2-hydroxyethyl)-1-piperazineethanesulfonic acid
IMAGE	<b>I</b> ntegrated <b>M</b> olecular <b>A</b> nalysis of <b>G</b> enomes and their <b>E</b> xpression
IPTG	isopropyl- $\beta$ -D-thiogalactopyranoside
Kan	kanamycin
KLH	keyhole limpet hemocyanin
kDa	kiloDalton
L	leucine
LC-ESI-MS/MS	liquid chromatography-electrospray ionization-tandem mass spectrometry
L	liter
LB	Luria-Bertani medium
K	lysine
LAMP1	lysosomal-associated membrane protein 1
Mg	magnesium

Mn	manganese
MS	mass spectrometry
MALDI	Matrix-assisted laser desorption/ionization
$V_{\max}$	maximum velocity
$K_m$	Michaelis constant
um	micrometer
uM	micromolar
mg	milligram
ml	milliliter
mM	millimolar
MGYH	minimal glycerol + histidine medium
MMH	minimal methanol + histidine medium
min	minutes
M	molar
MW	molecular weight
NEM	N, N'-ortho-phenylenedimaleimide
Ni	nickel
NAD	nicotinamide adenine dinucleotide, oxidized form
NADH	nicotinamide adenine dinucleotide, reduced form
NMT	N-myristoyltransferase
<i>Nco</i>	<i>Nocardia corallina</i>

NFM	non-fat milk
OD <sub>600</sub>	optical density at 600 nanometers
O	oxygen
PMSF	phenylmethylsulfonyl fluoride
P <sub>i</sub>	phosphate
PBS	phosphate-buffered saline
<i>P. pastoris</i>	<i>Pichia pastoris</i>
PAGE	polyacrylamide gel electrophoresis
PCR	polymerase chain reaction
<i>P. mevalonii</i>	<i>Pseudomonas mevalonii</i>
<i>pfu</i>	<i>Pyrococcus furiosus</i>
RPI	research products international
rev	reverse
<i>R. rubrum</i>	<i>Rhodospirillum rubrum</i>
RT	room temperature
sec	second
S or Ser	serine
Na	sodium
<i>Sac</i>	<i>Streptomyces achromogenes</i>
S-tag	subtilisin cleavable tag
kpsi	thousand pounds per square inch
xg	times gravity

TIM	triosephosphate isomerase
TBS	tris-buffered saline
TBST	tris-buffered saline with 0.1% Tween-20
<sup>3</sup> H	tritium
TX-100	triton X-100
U	unit
V	valine
V	volt
WT	wild-type
<i>Xho</i>	<i>Xanthomonas holcicola</i>
YPD	yeast extract peptone dextrose medium

## ACKNOWLEDGMENTS

I would like to thank Dr. Henry Miziorko for taking a chance on a less than ideal student. Dr. Miziorko supplied guidance and support while allowing me to try doing things in new ways. I would also like to thank my committee members Dr. Marilyn Yoder, Dr. Anthony Persechini, Dr. Karen Bame, and Dr. Brian Geisbrecht for not only pointing out the flaws in my work, but also the successes. I like to thank the members of the Miziorko lab as well. Dr. Timothy Herdendorf got me started in the lab, Dr. Natalia Voynova taught me to do things by the book, and Dr. Andrew Skaff reminded me that not everything can be done by the book. I would especially like to thank Dr. Paul Watkins and the members of his lab for their years of collaboration on the localization of HMGCLL1 and for allowing me to spend some time working in their lab. My parents, Nancy and John Kishpaugh, and my Grandparents Leonard and Irma Cochran were always there to listen to me when every thing was going wrong and always knew that it was going to work out. I would like to thank my older children, Dylan, Heather, Lucian, and Zoe for understanding why I couldn't "just work at McDonald's or WalMart like other mommies do". I hope that when they are old enough, my youngest children Evan and Rowan will forgive me for spending so much time at the lab and in the study. Last but not certainly not least, I would like to thank my husband for understanding why I had to go back to school and for being a taxi driver, maid, cook, and nanny while I did.

## CHAPTER 1

### INTRODUCTION

#### Ketogenesis

Ketogenesis is the process by which acetyl-CoA is converted to the ketone bodies 3-hydroxybutyric acid (3HB), acetoacetic acid (AcAc), or acetone (Figure 1.1). Catabolism of the amino acids phenylalanine, tyrosine, isoleucine, leucine, lysine, tryptophan, and threonine can contribute to ketogenesis directly by yielding acetoacetate or indirectly via acetyl-CoA. However, the primary source of acetyl-CoA for the production of ketone bodies is beta oxidation of fatty acids (1). Since the brain cannot efficiently utilize circulating fatty acids for energy (2), ketone bodies become an important source of energy for the brain when supplies of glucose, its preferred energy source, are low (3).

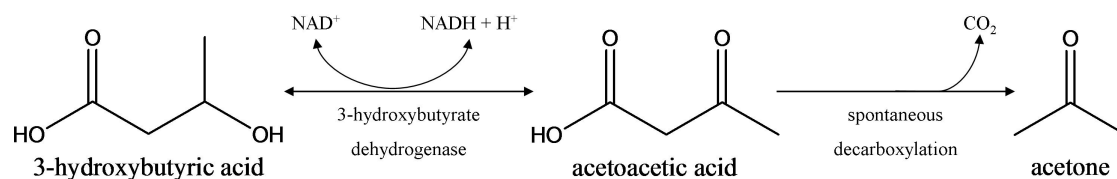


Figure 1.1. Structures of the ketone bodies. Both 3-hydroxybutyric acid (3HB) and acetone are derived from acetoacetic acid (AcAc). Acetone is produced by spontaneous decarboxylation of AcAc. 3-hydroxybutyric acid is formed by the enzymatic reduction of AcAc by 3-hydroxybutyrate dehydrogenase (3HBDH).

Acetoacetic acid production occurs primarily within hepatocyte mitochondria (4) in three enzymatic steps (Figure 1.2). A fourth enzymatic step interconverts AcAc and 3HB. The first step, condensation of two acetyl-CoA molecules to form acetoacetyl-CoA, is catalyzed by acetyl-CoA acetyltransferase. The rate limiting step, catalyzed by

3-hydroxy-3-methylglutaryl-CoA synthase (HMG-CoA synthase), produces 3-hydroxy-3-methylglutaryl-CoA (HMG-CoA) from the condensation of a third acetyl-CoA with acetoacetyl-CoA. Isoforms of both acetyl-CoA acetyltransferase and HMG-CoA synthase can also be found in the cytosol where they initiate the cholesterol synthesis pathway. The third step, cleavage of HMG-CoA to form the ketone body acetoacetic acid (AcAc) and acetyl-CoA, is catalyzed by 3-hydroxy-3-methylglutaryl-CoenzymeA lyase (HMG-CoA lyase). Acetoacetic acid is volatile and can spontaneously decarboxylate to form acetone. Acetone has little metabolic significance; however, the fruity odor it imparts the breath is clinical indicator of ketosis. Finally, 3-hydroxybutyrate dehydrogenase catalyzes the interconversion of AcAc into the more stable 3-hydroxybutyric acid (3HB) whose only metabolic fate is interconversion with AcAc. This interconversion requires the cofactor  $\text{NAD}^+/\text{NADH}$  and the ratio of circulating 3HB to AcAc can be used as an indicator of mitochondrial redox potential.

### **Regulation of Ketogenesis**

Ketogenesis is regulated by controlling the supply of circulating fatty acids, the entry of those fatty acids into liver mitochondria, and conversion of acetyl-CoA into ketone bodies within the mitochondria. Fatty acid release from adipose tissue is primarily dependent on the action of hormone-sensitive lipase (HSL) which catalyzes the conversion of triglycerols to monoacylglycerols and free fatty acids. Increased levels of HSL transcripts are found during fasting while glucose and insulin suppress transcription. In the short term, activity of HSL can also be hormonally controlled by phosphorylation at several serines. Epinephrine or glucagon initiates a phosphorylation cascade that

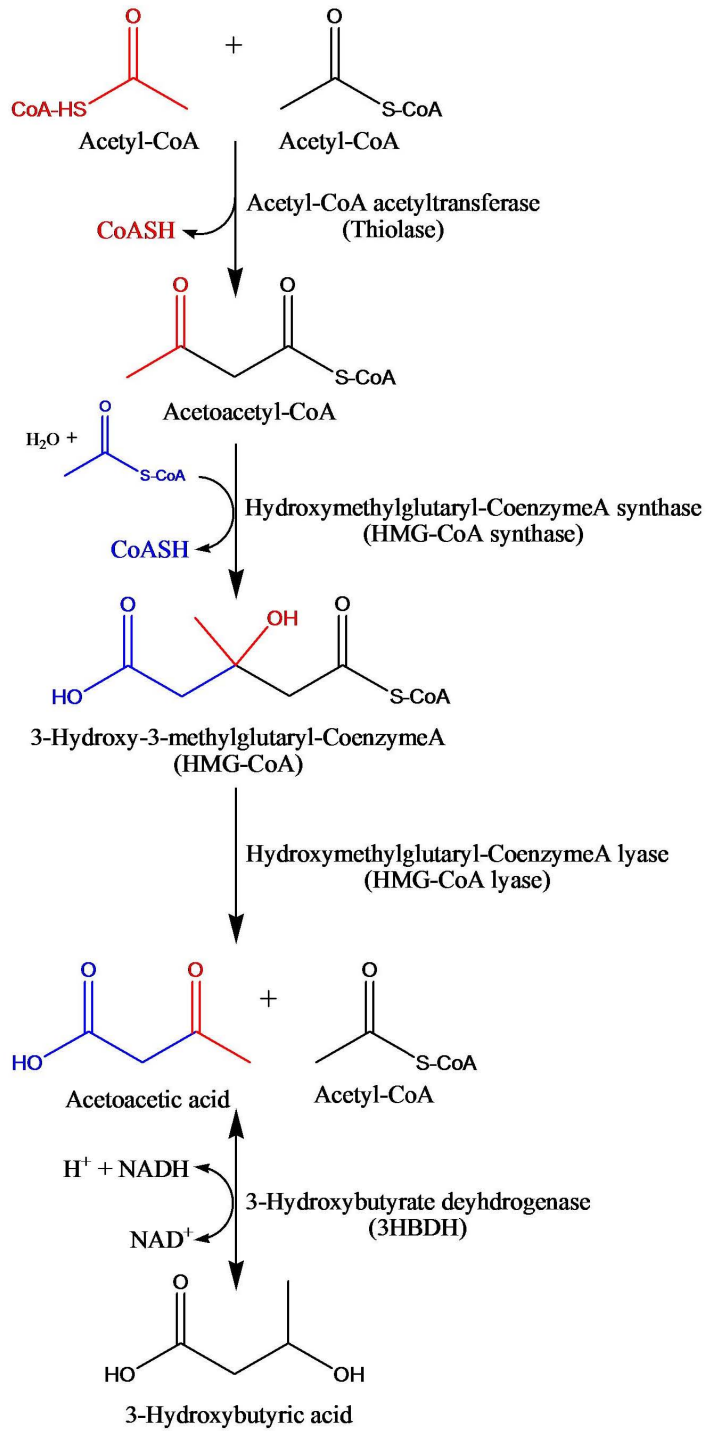


Figure 1.2. The enzymatic steps of ketogenesis.

activates HSL while insulin may activate phosphodiesterase 3B, causing dephosphorylation and thus inactivation of HSL. (5) Fatty acid entry into hepatic mitochondria is regulated at the first of three steps, transfer of a fatty acyl group from cytosolic acyl-CoA to carnitine catalyzed by the outer mitochondrial membrane protein carnitine palmitoyl transferase I (CPTI). Carnitine palmitoyl transferase I is inhibited by malonyl-CoA, the product of the first committed step in fatty acid synthesis. (6) Since acetyl-CoA carboxylase, which produces malonyl-CoA, is inhibited by palmitoyl-CoA and glucagon stimulated phosphorylation and is activated by citrate and insulin, CPTI is indirectly sensitive to feeding/fasting. Finally, conversion of acetyl-CoA to acetoacetate is regulated by control of mitochondrial HMG-CoA synthase. Transcripts of this enzyme are increased by glucagon, fat feeding, or diabetes and are decreased by insulin. (7) Post-translationally HMG-CoA synthase is inhibited by auto-succinylation in the presence of succinyl-CoA. (8) In summary, insulin (feeding) blocks ketogenesis by inhibiting HSL and HMG-CoA synthase and stimulating acetyl-CoA carboxylase causing a decrease in fatty acid availability, reducing the conversion of acetyl-CoA into acetoacetate, and blocking fatty acid entry into the mitochondria while glucagon (fasting) has the opposite effect (Table 1.1).

### **3-Hydroxy-3-methylglutaryl-CoenzymeA lyase**

3-Hydroxy-3-methylglutaryl-CoenzymeA lyase (HMG-CoA lyase or HMGCL) catalyzes the cleavage of HMG-CoA into the ketone acetoacetate and acetyl-CoA (9). This reaction is the final step in leucine and lysine catabolism and an important step in ketogenesis. Genes coding for HMGCL have been found in animals (from humans to

Table 1.1. Effects of Insulin and Glucagon on Key Enzymes Controlling Ketogenesis (10)

Enzyme	Location	Action	Result	Effect of insulin (decreases ketogenesis)	Effect of glucagon (increases ketogenesis)
Hormone sensitive lipase	Peripheral adipocytes	Breaks down triglycerides into fatty acids	Elevated serum fatty acids	Inhibited	Stimulated
Acetyl-CoA carboxylase	Hepatocytes (cytosolic)	Converts acetyl-CoA to malonyl-CoA	Malonyl-CoA blocks fatty acid entry into mitochondria (inhibits CPTI)	Stimulated	Inhibited
HMG-CoA synthase	Hepatic mitochondria	Converts acetoacetyl-CoA into HMG-CoA	Rate limiting step in producing acetoacetate	Inhibited	Stimulated

protozoans), plants, and bacteria. The recombinant forms of human (11), *Pseudomonas aeruginosa* (12), and *Bacillus subtilis* (Christa Montgomery, unpublished data) HMGCL as well as endogenous enzymes from bovine liver (13), avian liver (14), *Tetrahymena pyriformis* (protozoan) (15), and *Pseudomonas mevalonii* (16) have been purified and characterized (Table 1.2). All HMG-CoA lyases characterized to date absolutely require a divalent cation for activity ( $Mg^{2+}$  is preferred) and their activity is stimulated by

sulfhydryl reagents. The crystal structures of recombinant human (17), *Brucella melitensis*, and *Bacillus subtilis* (18) proteins have been solved, confirming a  $(\beta/\alpha)_8$  triosephosphate isomerase (TIM) barrel motif.

Table 1.2. Characteristics of HMG-CoA Lyases

Organism	Specific Activity ( $\mu\text{mol min}^{-1} \text{mg}^{-1}$ )	$K_m$ HMG-CoA ( $\mu\text{M}$ )	DTT Stimulation of Activity	Optimal pH
Recombinant Human (11)	159	25	10 fold	ND
Recombinant Human C323S (11)	348	45	10 fold	ND
Bovine Liver (13)	46	8	22 fold	9.5
Avian Liver (14)	350	8	100 fold	8.9
<i>Tetrahymena Pyriformis</i> (15)	431	15	Slight	9.0
<i>Pseudomonas aeruginosa</i> (12)	21	100	ND	7
<i>Pseudomonas mevalonii</i> (16)	ND	100	Modest	8.8
<i>Bacillus Subtilis</i> (Christa Montgomery, Unpublished data)	18	4.5	3 fold	ND

The human HMG-CoA lyase gene consists of 9 exons and has been mapped to chromosome 1p36.1-p35 spanning about 23.6 Kb (19). Although a comprehensive Northern blot analysis of transcript expression has not been done, transcripts have been detected in human fibroblasts, liver, and lymphoblasts (20) and HMG-CoA lyase activity has been described in liver, kidney, and heart (21). Full-length human HMG-CoA lyase contains 325 amino acids including a 27 residue N-terminal mitochondrial leader sequence and a C-terminal CK/RL type-1 peroxisomal targeting motif (22). Upon entry into the mitochondria, the mitochondrial leader sequence is cleaved producing the 298 residue mature mitochondrial lyase while a distinct, full-length form is present in peroxisomes (23).

### **HMG-CoA Lyase Deficiency**

HMG-CoA lyase deficiency highlights the importance of the ketogenic pathway. In humans, this disorder is autosomal recessively inherited (24) and in some areas represents up to 16% of hereditary metabolic disease (25). Lyase deficiency is fatal in about 20% of cases with acute crises occurring during fasting, illness, and exercise (26). HMG-CoA lyase deficiency can cause vomiting, dehydration, diarrhea, organic acid acidosis, hypoglycemia, decreased levels of consciousness, and coma (27). In some cases fever, seizures, an enlarged liver that functions abnormally, and abnormal cerebral white matter foci have been reported (28). The seriousness of this disorder has prompted previous investigations of a potential regulatory mechanism (29) which this work attempts to clarify and expand upon.

## CHAPTER 2

### INFLUENCE OF MULTIPLE CYSTEINES ON HUMAN HMG-COA LYASE ACTIVITY AND FORMATION OF INTERSUBUNIT ADDUCTS

#### **Introduction**

HMGCL activity is absolutely dependent on the presence of a divalent cation (e.g.  $Mg^{2+}$ ,  $Mn^{2+}$ ) and activity is stimulated by reducing agents (e.g. DTT). The influence of reducing agents may be explained by the observation that animal HMGCL proteins contain eight cysteine residues (30). Affinity labeling results (31) identified one of these residues (C266) as an active site residue in the avian enzyme. This residue is located in a flexible loop positioned over the active site (32, 33) and catalysis would be blocked if C266 mobility was constrained by participation in any disulfide adduct, providing a clear rationale for the enzyme's reducing agent requirement. Additionally, the sensitivity of one or more HMGCL cysteines to diminution in cellular reductant levels was suggested by observations that multiple physiological perturbations occur in a superoxide dismutase knock out mouse (34). These include a decrease in HMGCL activity and a consequent organic aciduria due to degradation of the pool of accumulating HMG-CoA metabolite.

Endogenously expressed enzyme, purified from avian liver tissue (35), was employed in protein chemistry experiments which demonstrated that the dimeric enzyme (32 kDa subunits) forms a covalent intersubunit adduct upon treatment with the sulfhydryl selective reagent, *N, N'*-ortho-phenylenedimaleimide (36). Difference peptide maps of tryptic digests prepared from crosslinked and non-crosslinked proteins implicated two peptides as harboring the modification targets. Edman degradation and amino acid

composition analyses demonstrated that these are related, C-terminal region peptides which correspond either to residues 318-324 (VSQAACR) or residues 318-325 (VSQAACRL). The simplest explanation for all data available at that time involved the hypothesis that an intersubunit crosslink formed between a C-terminal C323 residue from each subunit of the dimeric enzyme. When a recombinant form of human HMGCL became available, wild-type and C323S proteins were used to extend studies on the effects of reducing agents and cysteine selective protein crosslinkers (37). Results of these studies, which focused only on the function of C323, were consistent with the proposed role for a C-terminal cysteine in formation of a covalent intersubunit adduct.

Subsequently, the 2.1 Å resolution crystal structure of human HMGCL became available (38). The structure did not clearly identify cysteines (including C323) that would participate in formation of the interchain adduct observed upon disulfide formation or chemical crosslinking (39, 40). These observations suggested that it would be informative to expand the investigation to include the possible contribution of other cysteine residues in formation of either *intrasubunit* or *intersubunit* covalent adducts. The results of these studies suggest that multiple cysteine residues influence covalent adduct formation in HMG-CoA lyase as well as the dependence of enzyme activity on reducing agent.

## **Materials and Methods**

### **Materials**

*E. coli* JM109 and BL21 competent cells, miniprep, midiprep, and gel purification kits were purchased from Promega. dNTPs and Pfu DNA polymerase used for

mutagenesis were purchased from Stratagene. Primers used for mutagenesis were synthesized by Integrated DNA Technologies. *BamHI*, *NcoI*, and *DpnI* endonucleases were obtained from New England Biolabs. DNA sequencing was performed at the DNA Core Facility, University of Missouri-Columbia. Ni-Sepharose was purchased from GE Healthcare, Bradford reagent and unstained protein standards from Bio-Rad, NEM from Eastman-Kodak, ECL reagents and PMSF from Pierce, and autoradiography film from MIDSCI (St. Louis, MO). Secondary antibodies, Tween 20, NAD, NADH, malic acid, and coupling enzymes were purchased from Sigma-Aldrich. DNA ligase, DNase I, media components, buffers, DTT, and all other reagents were obtained from Fisher Scientific.

#### Plasmid Construction

The open reading frame encoding the mature mitochondrial form of human HMGCL was sub-cloned into the expression vector pET30b (Novagen) using standard molecular biology techniques. Briefly, the HMGCL coding sequence was excised from pTrc99 HL (41) using the restriction endonucleases *BamHI* and *NcoI* and gel purified. The purified restriction fragment was ligated with a similarly digested and purified pET30b vector. The ligation produced an expression construct, pET30HL, which encodes mature mitochondrial HMGCL containing N-terminal His<sub>6</sub> and S-tags. DNA sequence analysis was used to verify the integrity of the final product.

#### Protein Expression

Chemically competent *E. coli* BL21 (DE3) cells (Promega) were transformed with pET30HL, plated onto LB agar containing 50 µg/ml kanamycin (Kan), and incubated

overnight at 37°C. A single colony was used to inoculate 6 ml of LB/Kan for overnight growth. Glycerol stocks were made from the overnight culture by combining 1 ml of culture with 0.5 ml of sterile 50% (v/v) glycerol and storing at -80°C. A 50 ml starter culture of LB/Kan was inoculated from glycerol stock, incubated overnight at 37°C, and 2-3 ml used to inoculate a 1 L culture of LB/Kan. After incubation at 37°C until the OD<sub>600</sub> was 0.5 – 0.6, protein expression was induced by the addition of sterile IPTG (RPI; final concentration, 1 mM). After overnight incubation at 22°C, the induced cells were harvested by centrifugation and pellets were stored at -80°C until protein purification. Similar conditions were used for the expression of mutant proteins.

### Mutagenesis

Mutants were generated using full circle PCR according to Stratagene's QuickChange site-directed mutagenesis protocol. The WT pET30HL construct was used as a template for single mutants and the pET30HL C170S mutant construct was used as a template for double mutants. Mutations were verified by DNA sequence analysis. Forward and reverse mutagenic primer sequences (mutagenic bases underlined) are as follows:

C141S for: 5'- CCAAGAAGAACATCAATAGTTCCATAGAGGAGAG -3'

C141S rev: 5'- CTCTCCTCTATGGAACTATTGATGTTCTTCTTGG -3'

C170S for: 5'- GGTACGTCTCCTCTGCTCTTGGCTGC -3'

C170S rev: 5'- GCAGCCAAGAGCAGAGGAGACGTACC -3'

C174S for: 5'- CCTGTGCTCTTGGCAGCCCTTATGAAGGG -3'

C174S rev: 5'- CCCTTCATAAGGGCTGCCAAGAGCACAGG -3'

C197S for: 5'- CTACTCAATGGGCTCTACGAGATCTCCCTGG -3'

C197S rev: 5'- CCAGGGAGATCTCGTAGGAGCCCATTGAGTAG -3'

C234S for: 5'- CCTGGCTGTCCACTCCCATGACACCTATGG -3'

C234S rev: 5'- CCATAGGTGTCATGGGAGTGGACAGCCAGG -3'

C266S for: 5'- GGACTTGGAGGCTCTCCCTACGCACAGG -3'

C266S rev: 5'- CCTGTGCGTAGGGAGAGCCTCCAAGTCC -3'

C307S for: 5'- GCTGGAAACTTTATCTCTCAAGCCCTGAACAG -3'

C307S rev: 5'- CTGTTCAGGGCTTGAGAGATAAAGTTTCCAGC -3'

C323S for: 5'- GGCTCAGGCTACCTCTAAACTCTAGGATCCG -3'

C323S rev: 5'- CGGATCCTAGAGTTTAGAGGTAGCCTGAGCC -3'

#### Enzyme Purification

All steps were carried out at 4°C. Bacterial pellets from 1 L of expression culture were resuspended in 100 ml of ice cold lysis buffer containing 50 mM NaP<sub>i</sub> (pH 7.8), 300 mM NaCl, 5% (v/v) glycerol, and 5 mM imidazole. Protease inhibitors (1 mM PMSF, 1 μM pepstatinA, and 10 μM leupeptin), 1 U/ml DNaseI, and 5mM mercaptoethanol were added immediately before cell disruption. Cells were mechanically disrupted by passing twice through a microfluidizer at ~17 kpsi. The lysate was clarified by centrifugation at 10,000 xg for 10 min. and the supernatant was loaded onto Ni-Sepharose Fast Flow resin (~1 ml). The column was washed with 50 mM NaP<sub>i</sub> (pH 7.8), 300 mM NaCl, 10% (v/v) glycerol, 40 mM imidazole, and 5 mM mercaptoethanol until the A<sub>280</sub> < 0.010. The protein was eluted slowly overnight with 50 mM NaP<sub>i</sub> (pH 7.8), 300 mM NaCl, 20% (v/v) glycerol, 300 mM imidazole and 5 mM mercaptoethanol. Fractions containing HMGCL were pooled and the concentration was determined by the method of Bradford

(42). The homogeneous wild type enzyme was found to have a  $V_{max}$  of 123 U/mg and a  $K_m$  for HMG-CoA of 26  $\mu$ M, values which are comparable with those for pTrc99 HL-expressed enzyme. These conditions were also utilized for the purification of mutant proteins.

### Enzyme Activity Measurement

Enzyme activity was determined using the method of Stegink and Coon (43) as modified by Kramer and Mizioroko (44). HMG-CoA was synthesized using the method of Goldfarb and Pitot (45). Briefly, this spectrophotometric assay couples the acetyl-CoA produced upon the cleavage of HMG-CoA to the reactions of malate dehydrogenase and citrate synthase. For each acetyl-CoA that condenses with oxaloacetate to form citrate, one malate is oxidized to oxaloacetate, producing one NADH. The rate of NADH production is determined by measuring the increase in  $A_{340}$  and is proportional to the amount of HMG-CoA lyase added. DTT was omitted from assays of nonreduced enzyme but included at 5 mM levels in measuring activity under reducing conditions.

### Preparation of Nonreduced Enzyme

Since buffer exchange via gel filtration, centrifugal ultrafiltration, or dilution resulted in variability in measured activity and levels of covalently linked dimer in nonreduced enzyme, extensive dialysis was employed to fully deplete reducing agents, permitting spontaneous formation of disulfide linkages. Purified protein was diluted in cold, air equilibrated, non-reducing dialysis buffer consisting of 50 mM  $\text{NaP}_i$  (pH 6.8), 100 mM NaCl, and 20% (v/v) glycerol to a concentration of 1 mg/ml. A volume < 1 ml of protein was dialyzed against 4 L of buffer for at least 16 hrs at 4°C. Longer dialysis and/or

multiple exchanges of buffer did not increase the enzyme's dependence on thiol for activity or intensity of the dimer band upon SDS-PAGE analysis.

#### NEM Modification

Free enzyme thiols were alkylated with NEM to prevent thiol-disulfide exchange upon denaturation. Small aliquots of reduced or nonreduced dialyzed protein were diluted into reaction mixtures containing final concentrations of 100 mM NaP<sub>i</sub> (pH 6.8) and 100 mM NEM. After 10 minutes, SDS was added to a concentration of 0.05% (w/v) to unfold protein and maximize NEM modification. Reactions were allowed to proceed at 23°C for an additional 60-90 minutes. Longer incubation times resulted in some formation of non-reducible protein dimer.

#### SDS-PAGE and Western Blotting

SDS-PAGE was performed using a 12% resolving gel and a 4% stacking gel as described by Laemmli (46). For reducing gels, samples were heated (95°C) for 5 min. in loading buffer containing a minimum of 50 mM mercaptoethanol. For nonreducing gels, samples were prepared as above except mercaptoethanol was omitted from the loading buffer. Protein bands were visualized using Coomassie blue staining. In Western blot experiments, proteins were transblotted from SDS-PAGE gels to nitrocellulose overnight at 23V at 4°C. Blots were blocked in 5% (w/v) non-fat milk (NFM) dissolved in tris-buffered saline with 0.1% (v/v) Tween-20 (TTBS) for 30 min. at room temperature (RT) with agitation. Blots were incubated in a 1:5000 dilution of rabbit anti-HMGCL serum in 3% (w/v) NFM/TTBS for 1 hr. at RT. Rinsed blots were then incubated in a 1:10,000 dilution of horseradish peroxidase conjugated goat anti-rabbit IgG in 3% NFM/TTBS for

1 hr. at RT. Finally, rinsed blots were incubated for 5 min. at RT in enhanced chemiluminescence (ECL) Western Blotting Substrate (single mutants) or West Pico ECL Substrate (double mutants), and exposed to autoradiology film for 5 min. in a darkroom. A Bio-Rad or Fermentas PageRuler Plus prestained protein ladder was used to estimate molecular weights.

## Results

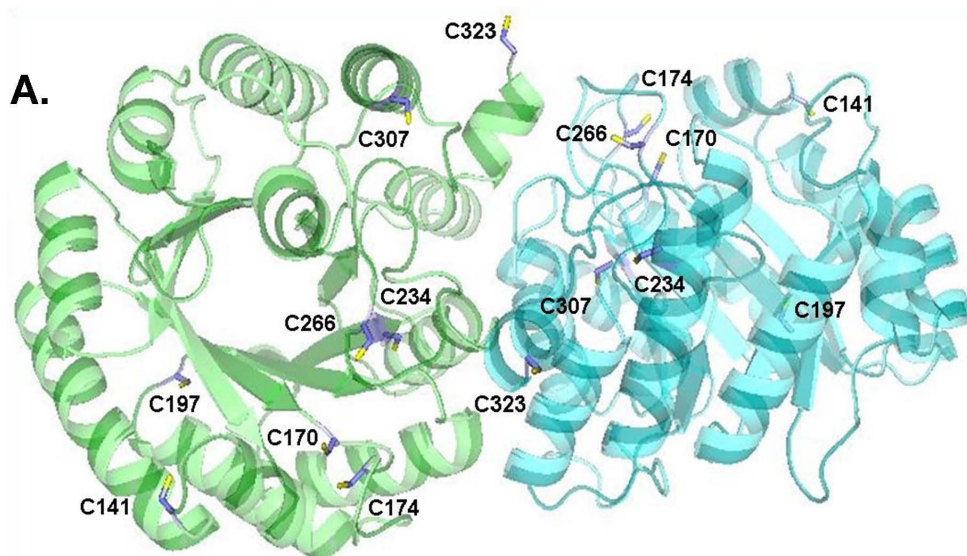
### Location of Cysteine Residues in Native Human HMGCL

Human HMGCL (RCSB coordinates 2CW6)<sup>1</sup> crystallizes with six monomers in the asymmetric unit. The protein exhibits a  $(\beta/\alpha)_8$  barrel fold, with a highly conserved signature sequence (harboring C266) located in a very dynamic loop situated over the C-terminal end of the barrel. For two of the six monomers in the asymmetric unit, this loop is disordered, suggesting that it is highly flexible in solution. Nevertheless, the published data (47) make possible mapping the position of each of the eight cysteines in each subunit of the physiologically relevant dimer (Figure 2.1A). Using this structural model, it is possible to determine the distances between the different cysteine sulfhydryls that would have to be spanned if any intrachain (Figure 2.1B) or interchain (Figure 2.1C) covalent (e.g. disulfide) adduct was to be formed. For intrachain interactions, there are three sulfur-sulfur pair distances that are in the 4-10 Å range (C170/C174; C266/C170; C266/C174). For interchain interactions, two sulfur-sulfur pair distances (C234/C234; C266/C323) are in the 13-20 Å range. Formation of a C170/C174 intrachain disulfide

---

<sup>1</sup> The structure of enzyme without substrate or inhibitor acyl-CoA ligands (only bound  $Mg^{2+}$  and 3-hydroxyglutarate) is the appropriate model for the protein samples used in these studies.

Figure 2.1. Crystal structure of HMGCL and distances between cysteine sulfurs. Panel A displays a Pymol (48) ribbon drawing representation of the crystal structure of human HMGCL (2CW6) which was solved at a resolution of 2.1 Å (49). The physiological dimer consists of two  $(\beta/\alpha)_8$  TIM barrels, oriented with the axes of the two barrels perpendicular to each other. This structure contains no bound acyl-CoA substrate or inhibitor; one chain (A) is occupied by bound  $Mg^{2+}$  and 3-hydroxyglutarate, which indicate the active site at the C-terminal end of the barrel. The view of the monomer on the left is from the C-terminal end of the barrel cavity. The barrel of the monomer on the right is rotated by about  $90^0$  relative to the left monomer. Interchain and intrachain distances between HMGCL cysteines are displayed in panels B and C, respectively. The Swiss PDB viewer Deep View (4.01) (50) was used to determine the distance (in Angstroms) between each cysteine sulfur of the physiological HMGCL dimer. The shortest intrachain distances are highlighted in the upper table. Highlighted in the lower table are the shortest interchain and the shortest homo-disulfide distances.



**B.**

		Intrachain							
		Chain B (empty active site)							
		C141	C170	C174	C197	C234	C266	C307	C323
Chain A (HMG in active site)	C141		14.5	15.2	16.3	25.6	22.8	34.6	47.7
	C170	13.3		3.9	17.3	13.2	11.4	26.6	38.3
	C174	14.0	4.1		20.6	16.1	12.3	28.9	40.6
	C197	15.5	17.1	20.6		19.0	24.9	31.2	41.9
	C234	24.7	13.5	16.5	19.0		13.6	20.9	29.2
	C266	18.0	8.3	10.1	21.0	13.1		17.8	29.3
	C307	34.3	26.6	29.3	31.0	20.7	19.3		13.8
	C323	47.2	38.3	40.9	41.8	29.0	31.5	13.6	

**C.**

		Interchain							
		Chain B (empty active site)							
		C141	C170	C174	C197	C234	C266	C307	C323
Chain A (HMG in active site)	C141	68.6	55.1	56.4	61.5	43.9	48.0	41.9	32.1
	C170	56.1		44.8	48.3	31.2	36.4	30.7	22.2
	C174	57.4	44.9		49.0	32.8	38.2	30.3	20.8
	C197	62.6	48.3	47.5		38.3	43.1	43.1	37.8
	C234	44.8	31.0	32.4	38.2		25.9	26.1	24.8
	C266	51.9	39.0	39.6	46.2	28.6		24.3	17.0
	C307	42.6	30.1	29.5	43.2	26.1	20.0		25.0
	C323	33.0	22.4	21.2	38.3	25.0	13.7	25.0	

adduct seems likely on the basis of close proximity but a multiplicity of such adducts could result if dynamics of the C266-containing loop or other mobile cysteine-containing structural regions close the distances between pairing partners.

### Reduction of Microheterogeneity in SDS PAGE Mobility Upon

#### N-Ethylmaleimide Modification of Nonreduced HMGCL

Sequence alignment of a diverse selection of eukaryotic and prokaryotic HMGCL proteins (Figure 2.2) suggests that, among the eight residues of animal HMGCL proteins, only C266 (human sequence numbering) is invariant and C174 is very highly conserved. Calculated molecular mass for a monomer of the recombinant human protein produced using the pET30b expression construct is 36.6 kDa (in reasonable agreement with a MALDI estimate of 36.7 kDa); apparent mass calculated from SDS-PAGE mobility (Figure 2.3, lane 1) is 39 kDa. Some indication of the possible multiplicity of disulfide

	141	170/174	197	234	266	307	323
<i>H. sapiens</i>	INCSI	CALGCPYE	MGCYE	VHCHD	VAGLGGCPYA	FICQA	ATCKL
<i>G. gallus</i>	INCSI	CVLGCPYE	MGCYE	VHCHD	VAGLGGCPYA	FICNA	AAQRL
<i>D. melanogaster</i>	VNCTA	TVVGCPE	MGCYE	VHCHD	VSGLGGCPYA	YICTE	ARVK-
<i>P. mevalonii</i>	INCSI	CVLGCPFS	LGCEY	GHFHD	VAGLGGCPYS	ALCQT	RAGLA
<i>R. rubrum</i>	INCSI	CVLGCPYE	MGCHE	AHFHD	VAGLGGCPYA	ASRAA	-----
<i>B. subtilis</i>	INKST	TVFGCPYE	FGISE	LHFHD	AGGLGGCPYA	WIEEK	-----

Figure 2.2. Sequence alignment of diverse eukaryotic and prokaryotic HMG-CoA lyase proteins. Residues flanking cysteine residues in the animal proteins are depicted. Alignment was generated using ClustalW. Residue numbering corresponds to human HMGCL (uncleaved mitochondrial isoform). Sequences from the following organisms are included: *Homo sapiens*, *Gallus gallus*, *Drosophila melanogaster*, *Pseudomonas mevalonii*, *Rhodospirillum rubrum*, and *Bacillus subtilis*. Amino acid sequences were obtained from the UniProt database using the following accession numbers: P35914, P35915, Q9VM58, P13703, Q2RT05, and O34873 respectively.

bonds in nonreduced HMGCL is apparent upon comparison of such protein samples that are either unmodified or treated with N-ethylmaleimide (NEM) to modify any non-disulfide linked cysteines prior to sample analysis by SDS-PAGE. NEM blocking of accessible cysteines prior to and during sample denaturation reduces the possibility of additional new extraneous inter- or intra-chain disulfide formation. Also reduced is the exchange of available free cysteines with any existing disulfides in samples of nonreduced protein to form different disulfide linkages as the remaining cysteines become exposed. NEM sharpens the covalently linked dimer SDS-PAGE band (Figure 2.3, lane 5) that is otherwise quite diffuse and difficult to observe (Figure 2.3, lane 4). Similarly, the monomer band from the untreated nonreduced sample (Figure 2.3, lane 4) is more diffuse than observed for the sample which is NEM treated and subsequently reduced to eliminate any disulfide bonds prior to SDS-PAGE (Figure 2.3, lane 2). Such sharpening of the monomer band is compatible with the microheterogeneity that would be expected if intrasubunit disulfide linkages also form within the monomer of the nonreduced protein. Therefore, to optimize detection of covalent interchain adducts, as well as to sharpen monomer bands, NEM modification of free cysteines was routinely performed prior to and during denaturation of samples for analysis by SDS PAGE.

#### Strategy for Evaluation of Cysteine Residue Contributions to Disulfide

##### Bond Formation and to Enzyme Activity in the

##### Presence or Absence of Reductant

A mass spectrometry/proteomics (LC-ESI-MS/MS) approach was evaluated by preliminary experiments that identified and compared peptides from either tryptic or

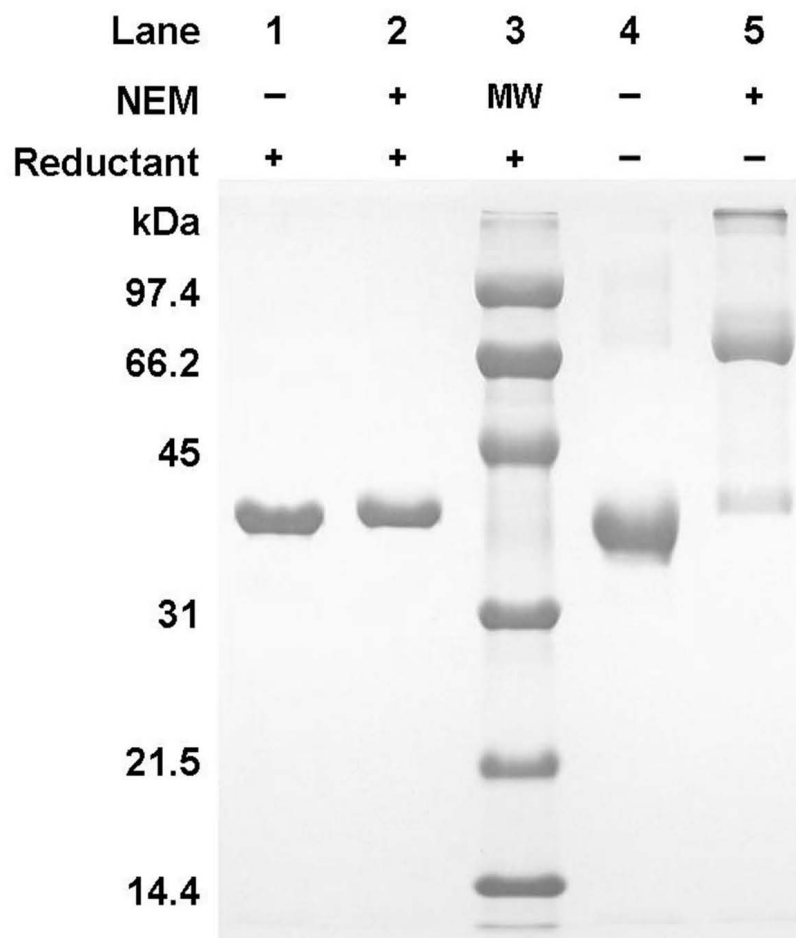


Figure 2.3. SDS-PAGE of human HMGCL under reducing or nonreducing conditions. Purified HMGCL was subjected to dialysis (>16 hr) in air equilibrated buffer. An aliquot was incubated with the sulfhydryl-specific alkylating reagent NEM (lanes 2, 5) while another aliquot was mock treated (lanes 1, 4). Reactions were split in half and denatured in an equal volume of SDS loading buffer and treated (lanes 1-3) or untreated (lanes 4-5) with mercaptoethanol (2%) prior to heating (95 °C) for 5 min. Five  $\mu$ g of protein was loaded in each lane of a 12% SDS-PAGE gel. Molecular weight markers (lane 3) include: phosphorylase b, 97.4 kDa; bovine serum albumin, 66.2 kDa; ovalbumin, 45 kDa; carbonic anhydrase, 31 kDa; trypsin inhibitor, 21.5 kDa; lysozyme, 14.4 kDa.

chymotryptic HMGCL digests. Tryptic and chymotryptic digests were prepared from samples of NEM modified HMGCL that were either reduced with DTT or untreated after extensive dialysis in air equilibrated buffer. Due to the high sensitivity of the MS approach and the presence of eight cysteine residues in HMGCL, widely ranging peak intensities attributable to various disulfide linked candidate peptides were detectable. Such observations characterized not only digests of nonreduced samples but also digests of NEM modified reduced control protein, which should only contain trace levels of disulfide linkages. The difficulty in accurately estimating relative abundance of candidate disulfide linked peptides for comparisons between samples complicated identification of functionally important disulfides. These developments prompted initiation of an alternate approach for a less ambiguous evaluation of the formation of disulfide adducts in nonreduced HMGCL as well as the influence of individual cysteines on the dependence of activity on exogenous reducing agents.

Site directed mutagenesis was employed to generate eight Cys→Ser mutant HMGCL proteins with a single substitution for each individual cysteine residue. The mutant proteins were expressed (pET30b constructs) at levels comparable to wild type enzyme. The soluble fractions of lysates containing these N-His-tagged proteins were purified by nickel affinity chromatography. Detection of monomeric and covalently linked dimeric enzyme bands after SDS-PAGE was performed on western blots using polyclonal rabbit antiserum prepared against avian liver enzyme (51). As described below, the mutant enzymes were suitable for both activity analyses as well as for detection of covalently linked dimers, validating the decision to pursue an expanded mutagenesis approach.

Additionally, the availability of the pET30b expression constructs (in addition to selected pTrc99 expression plasmids) for HMGCL mutant proteins enabled production of a C266/C323S heterodimer (*vide infra*). This protein supported an experimental test of the formation of a C266-C323 intersubunit adduct, which seemed plausible (*vide ante*) on the basis of structural proximity considerations (Figure 2.1C).

### Influence of Cysteine Substitutions on Intersubunit Adduct

#### Formation in Nonreduced Protein

When wild-type and each of the eight Cys→Ser mutant HMGCL proteins are reduced in the presence of 2% (v/v) mercaptoethanol prior to denaturing SDS-PAGE and Western blotting, each protein exhibits mobility expected for a monomer (Figure 2.4A). When samples of extensively dialyzed protein are not reduced prior to SDS-PAGE, interesting contrasts are apparent (Figure 2.4B). A substantial band corresponding to a covalently linked dimer of subunits is apparent for wild-type protein, as well as for C141S, C174S, and 307S mutant proteins; a dimer band of diminished intensity is also observed for C197S and C234S proteins. As previously reported for the pTrc99 expressed C323S protein (52), no dimer is observed for C323S protein. However, in extending this study to other Cys→Ser mutants, it now becomes clear that a dimer adduct is also undetectable in nonreduced samples of either C266S or C170S mutants. Thus, multiple cysteines (e.g. C170, C266, and C323) can strongly influence intersubunit adduct formation in nonreduced HMGCL. Such a possibility had not previously been considered.

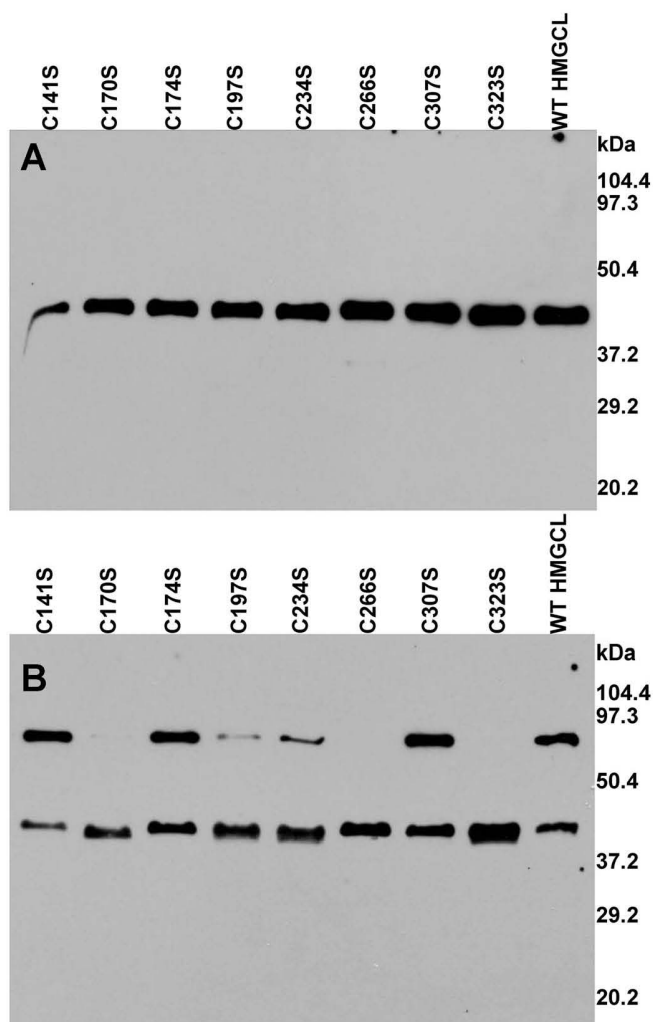


Figure 2.4. Western blots of human HMGCL Cys→Ser mutants under reducing [A] or nonreducing [B] conditions. Purified HMGCL and Cys→Ser mutants were dialyzed (>16 hr) in air equilibrated buffer. Free cysteines were alkylated with the sulfhydryl-specific reagent NEM prior to and during denaturation with SDS loading buffer. Equal volumes of each reaction were denatured in 2x SDS loading buffer and then incubated in the presence [A] or absence [B] of mercaptoethanol [2% (v/v)] prior to heating (95°C) for 5 min. Proteins (0.25 μg each except C197S, 0.75 μg) were run in separate lanes of two 12% SDS-PAGE gels and transblotted to nitrocellulose. Protein bands were detected as described in experimental procedures. Prestained molecular weight markers include: phosphorylase b, 104.4 kDa; bovine serum albumin, 97.3 kDa; ovalbumin, 50.4 kDa; carbonic anhydrase, 37.2 kDa; trypsin inhibitor, 29.2 kDa; lysozyme, 20.2 kDa. Positions indicated for pre-stained molecular weight standards are determined when exposed autoradiography film is overlaid on the western blot.

## Coexpression of HMGCL C266S and C323S Proteins Supports Formation of a Heterodimer that Forms a Covalent Intersubunit Adduct

*E. coli* BL21 (DE3) cells were transformed with both purified pET30 HL C266S and pTrc HL C323S plasmids. Double transformants were selected on LB agar plates containing both kanamycin (pET30 marker) and ampicillin (pTrc99 marker). After IPTG expression of HMGCL in a culture of a double transformant, a soluble lysate fraction which could include C266S homodimer, C323S homodimer, and/or C266S/C323S heterodimer was prepared. This sample was subjected to nickel sepharose chromatography. Any pTrc expressed C323S homodimer is untagged and elutes in unbound fractions. The affinity (imidazole) eluted protein includes dimeric enzyme containing at least one pET30 expressed his tagged C266S subunit. Any C266S homodimer in the affinity eluate will not exhibit significant catalytic activity (Table 2.1). The specific activity of the affinity eluted protein is >20-fold higher than attributable to C266S homodimer. This suggests elution of a heterodimeric species comprised of not only a his tagged, low activity C266S subunit but also an untagged C323S subunit, which retains high catalytic activity (53). Such a heterodimer should contain on one subunit a C266 sulfhydryl juxtaposed toward the adjacent subunit's C323 sulfhydryl (a potential disulfide forming residue pair; Figure 2.1A). Additionally, the heterodimer contains on adjacent subunits one pair of S266 and S323 residues. After extensive dialysis of the purified protein, nonreduced and reduced samples were subjected to SDS-PAGE and Western transfer. Immunodetection indicated the presence of a covalent HMGCL dimer attributable to C266S/C323S protein (Figure 2.5, lane 4) and, as expected, no covalent

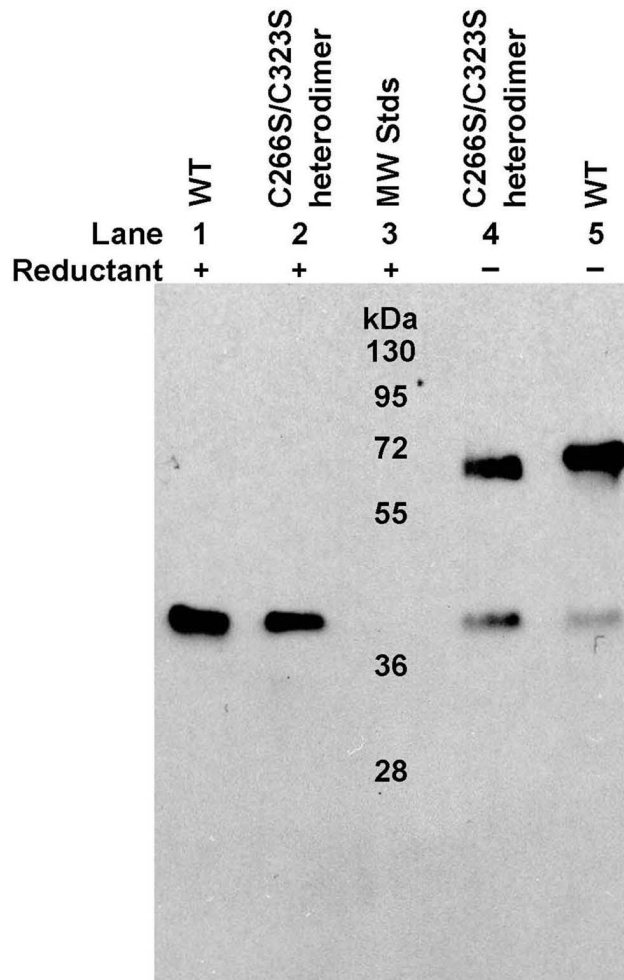


Figure 2.5. Western blot of human HMGCL and pET30HL C266S / pTrcHL C323S heterodimer under reducing and nonreducing conditions. Wild type HMGCL and pET30HL C266S / pTrcHL C323S heterodimer were extensively dialyzed (>16 hr) in air equilibrated buffer. Free cysteines were alkylated with the sulfhydryl-specific reagent NEM prior to and during denaturation with SDS loading buffer. Aliquots of each reaction were denatured in 2x SDS loading buffer and then incubated in the presence (lanes 1 and 2) or absence (lanes 4 and 5) of mercaptoethanol [2% (v/v)] prior to heating (95°C) for 5 min. Proteins (0.4 µg WT and 1 µg pET30HL C266S / pTrcHL C323S heterodimer) were run in separate lanes of a 12% SDS-PAGE gel and transblotted to nitrocellulose. Protein bands were detected as described in experimental procedures. The PageRuler Plus prestained protein ladder (Fermentas) was used to estimate molecular weights, as indicated in lane 3. The high molecular weight band in lane 4 is attributable to a heterodimeric form of HMGCL and is not observed (Figure 2.4) for either C266S or C323S homodimers.

dimer in any reduced HMGCL sample (Figure 2.5, lanes 1, 2). As already demonstrated in Figure 2.4, nonreduced C266S and C323S homodimers fail to form any covalent dimer. Thus, the detection of a covalent dimer, combined with the observation of catalytic activity in the nickel resin purified protein are most straightforwardly explained by formation of a heterodimer formed from one subunit containing a C266 sulfhydryl and another containing a C323 sulfhydryl. This empirical observation validates the prediction of such an adduct that was based on the proximity of these residues (Figure 2.1C) indicated by the X-ray structure of the enzyme.

#### Influence of Individual Cysteines on HMGCL Catalytic Activity

Previous studies on HMGCL cysteines were focused by the results of affinity labeling experiments (54) which implicated C266 as a residue important to catalytic function, an observation that was supported by results of mutagenesis experiments (55). A pET30b based expression plasmid offered improvements in yield and simplification of purification of N-his tagged HMGCL. Wild type enzyme prepared using this methodology exhibits (Table 2.1) specific activity (123 U/mg),  $K_m$  HMG-CoA (26  $\mu$ M) and DTT stimulation of activity (~10-fold) comparable to pTrc expressed enzyme used in previous work (56). A series of eight individual Cys→Ser mutant proteins was prepared; dialyzed samples of the purified mutants supported activity measurements on reduced and nonreduced forms of each protein (Table 2.1). The C266S mutant, which contains at the catalytic site a side chain alcohol of higher pK than the normal cysteine thiol of wild type enzyme, is diminished in specific activity by ~550 fold, as expected. None of the other reduced mutants exhibits more than a 6-fold change of specific activity, which

indicates some influence on, but no crucial role in, catalytic function. Their specific activity values range from 17-107% of wild type activity.

If dialyzed mutant enzymes are not pre-incubated with reductant prior to or during assay, activity is reduced for all of the enzymes to different extents, confirming the requirement for a reducing agent in order to optimize activity but also indicating that multiple cysteines contribute to the requirement. For the non-catalytic mutant proteins (i.e. excluding C266S which, regardless of the presence/absence of reductant, exhibits minimal activity due to disruption of reaction chemistry (57, 58), the relative ability of dialyzed enzyme to recover activity under reducing conditions is most noteworthy for C170S. The effect (Table 2.1) is much larger for C170S (636-fold) than for C323S (9.6-fold), even though nonreduced samples of both mutants fail to form a covalent dimeric adduct (Figure 2.4B). In comparison with C323S, C141S does form a covalent dimer; it exhibits a modest (~5 fold) stimulation of activity by DTT. From these contrasts, it seems apparent that HMGCL *activity* is not strictly correlated with the level of covalently linked dimer detected in denatured, nonreduced protein. Rebound in enzyme activity upon reduction is also substantial for C197S and C234S mutants. Nonreduced samples of both of these proteins exhibit covalent dimer formation that is somewhat diminished (Figure 2.4B) in comparison with observations for wild type, C141S, C174S, or C307S proteins. However, the collected assay results most clearly implicate C170, a previously uninvestigated residue, as a key residue in affecting HMGCL activity as the level of reduction of the protein changes.

Table 2.1. Dependence of Activity of Human HMGCL Single Cys→Ser Mutants on Exogenous Thiol

Enzyme	Activity Recovered Following Reduction of Dialyzed Enzyme (U/mg)	Activity Following Dialysis (U/mg)	Stimulation of Activity by Exogenous Thiol	Intersubunit Dimer Formation <sup>a</sup>
	Reducing Assay Conditions	Non-Reducing Assay Conditions		Non-Reducing Assay Conditions
WT HMGCL	123 (± 7)	11.5 (± 1.4)	10.7 fold	Moderate
C141S HL	42.0 (± 3.7)	8.83 (± 0.23)	4.76 fold	Strong
C170S HL	53.1 (± 8.3)	0.084 (± 0.012)	636 fold	None
C174S HL	42.1 (± 5.9)	2.66 (± 0.30)	15.8 fold	Moderate
C197S HL	21.2 (± 0.6)	0.141 (± 0.012)	150 fold	Weak
C234S HL	128 (± 6)	0.742 (± 0.062)	172 fold	Weak
C266S HL	0.224 (± 0.010)	0.137 (± 0.005)	1.63 fold	None
C307S HL	132 (± 5)	13.8 (± 0.1)	9.56 fold	Moderate
C323S HL	132 (± 2)	13.8 (± 1.6)	9.57 fold	None

<sup>a</sup>Strong indicates a SDS PAGE dimer band (Figure 2.4B) which is >65% of the total intensity in that lane; moderate, 34-65%; weak, <34%.

## Investigation of the Possible Interaction Between Cysteines C170 and C174 as an Influence on Formation of Intersubunit Dimer Adducts

In animal and plant HMGCL proteins, C170 and C174 are conserved but, while homologous residues are found in some bacterial forms of the protein, strict conservation across a broad spectrum of HMGCL proteins is not observed. Three residues separate these cysteines in human HMGCL so they do not conform to the CXXC motif (59) implicated in many enzymes sensitive to oxidation/reduction. Nonetheless, these sulfhydryls are separated by only ~4 Angstroms (Figure 2.1B; [60]) and the serine substitution in C170S strongly influenced both the HMGCL activity levels in reduced versus nonreduced protein and also the ability of nonreduced protein to form a covalent dimer. Therefore, the influence of C170 on interactions with C174 and formation of covalent adducts between subunits was examined by expression, purification, and partial characterization of the C170S/C174S double mutant. Double mutants involving C170 as well as other residues (C266, C233) that affect detection of intersubunit adducts were also prepared and studied in parallel experiments. Activity measurements on dialyzed purified double mutants indicate that the large dependence on reductant observed for C170S (636-fold stimulation) is minimized in C170S/C174S; the more modest 11.4 fold stimulation (Table 2.2) that is observed is closer to the effects observed for double mutants C170S/C266S (2.6-fold), C170S/C233S (27.9-fold), and for other single Cys→Ser mutants (Table 2.1). The possibility of C170-C174 interactions that was suggested by these results was also investigated by SDS-PAGE analysis of the double mutants under reducing/non-reducing conditions. The results (Figure 2.6) indicate that

the serine substitution of both C170 and C174 side chains restores some formation of the intersubunit dimer in nonreduced protein. In contrast, comparable samples of C170S/C266S and C170S/C323S lack any detectable covalent dimer adduct, as is the case for single mutants C170S, C266S, and C323S (Figure 2.4). Thus, the absence of a thiol at residues 170 and 174 not only diminishes the large stimulation of activity by reductant that is observed for C170S but also alters the remaining cysteine-cysteine interactions that influence the formation of a covalently linked dimer.

Table 2.2. Dependence of Activity of Human HMGCL Double Cys→Ser Mutants on Exogenous Thiol

Enzyme	Activity Recovered Following Reduction of Dialyzed Enzyme (U/mg)	Activity Following Dialysis (U/mg)	Stimulation of Activity by Exogenous Thiol	Intersubunit Dimer Formation <sup>a</sup>
	Reducing Assay Conditions	Non-Reducing Assay Conditions		Non-Reducing Assay Conditions
WT HMGCL	123 (± 7)	11.5 (± 1.4)	10.7 fold	Strong
C170S HL	53.1 (± 8.3)	0.084 (± 0.012)	636 fold	None
C170S/C174S HL	1.06 (± 0.01)	0.093 (± 0.022)	11.4 fold	Moderate
C170S/C266S HL	0.123 (± 0.021)	0.047 (± 0.008)	2.62 fold	None
C170S/C323S HL	18.5 (± 1.3)	0.662 (± 0.024)	27.9 fold	None

<sup>a</sup>Strong indicates a SDS PAGE dimer band (Figure 2.4B) which is >65% of the total intensity in that lane; moderate, 34-65%; weak, <34%.

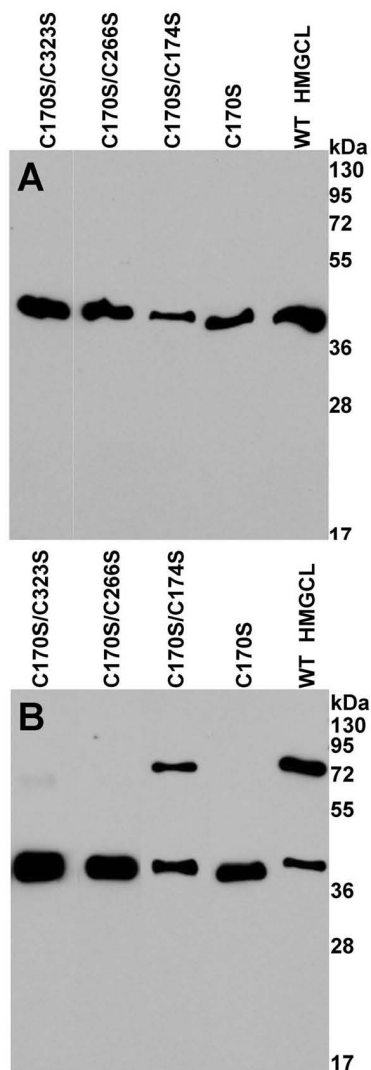


Figure 2.6. Western blots of human HMGCL C170S double mutants under reducing [A] or nonreducing [B] conditions. Purified HMGCL, C170S, and C170S double mutants were extensively dialyzed (16 hr) in air equilibrated buffer. Free cysteines were alkylated with the sulfhydryl-specific reagent NEM prior to and during denaturation with SDS loading buffer. Equal volumes of each reaction were denatured in 2x SDS loading buffer and then incubated in the presence [A] or absence [B] of mercaptoethanol [2% (v/v)] prior to heating (95°C) for 5 min. Proteins (0.13  $\mu$ g WT; 0.13  $\mu$ g C170S; 0.17  $\mu$ g [A] or 0.33  $\mu$ g [B] C170S/C174S; 0.17  $\mu$ g C170S/C266S, and 0.26  $\mu$ g C170S/C323S) were run in separate lanes of two 12% SDS-PAGE gels and transblotted to nitrocellulose. Protein bands were detected as described in experimental procedures. Positions indicated for pre-stained molecular weight standards are determined when exposed autoradiography film is overlaid on the western blot.

## Discussion

Magnitude of Dependence on Exogenous Reductants does not Correlate  
with Formation of Intersubunit Adducts.

HMGCL's requirement for a reducing agent in order to optimize activity had been previously attributed to the participation of C266 in catalysis and to C323's involvement in formation of the disulfide linked dimer in nonreduced C323S, which exhibits a diminution (~10-fold for recombinant protein) in activity. The absence of any interchain adduct after treatment of *Pseudomonas mevalonii* enzyme (which lacks a homologous C-terminal region cysteine; [61]) with a bifunctional chemical crosslinker (62) appeared to be consistent with the role proposed for avian HMGCL's C323. More recently, structural observations indicated that intersubunit disulfide linkages involving residues other than C323 (notably C266) required consideration due to their higher proximity to C323 on an adjacent subunit of the native enzyme dimer. The results of the more detailed experiments described above indicate that there is not any direct correlation between the formation of an intersubunit disulfide linked dimer in nonreduced protein and the magnitude of changes in HMGCL activity for reduced/nonreduced forms of wild type and mutant enzymes. For example, the magnitude of activity stimulation upon reduction of C323S, which forms no covalent intersubunit dimer, is comparable to activity stimulation observed for wild type enzyme, which does form such a dimer. A nonreduced sample of C170S, like C323S, shows no formation of covalent dimer (Figure 2.4B) but exhibits a very large activity stimulation upon DTT treatment (Table 2.1) in comparison with the effect observed for either wild-type or C323S enzymes. Comparisons of these

data with earlier observations are not complicated by the use of pTrc99 versus pET30b expressed protein. For samples subjected to dialysis in air equilibrated buffer, the magnitude of activity stimulation upon DTT treatment is comparable for HMGCL proteins produced by either expression method. Extended dialysis (>16 hours) with air equilibrated buffer produces pET30b expressed wild type enzyme that completely rebounds to its original activity level upon incubation with DTT. This observation agrees with earlier work using pTrc99 expressed enzyme, which employed a more rapid centrifugal gel filtration method to deplete residual reductant. The more extensive survey of the magnitude of sensitivity of each of eight cysteine substituted mutant enzymes to stimulation of activity upon reduction indicates that cysteines such as C197, C234 have intermediate effects on activity stimulation as well as the level of formation of covalently linked dimers. Such effects may indicate some possible involvement of these residues in disulfide exchange or in direct formation of intrasubunit disulfides but their influence is secondary to the larger effects discussed above in the context of C323S and C170S proteins.

#### Competition for C266 may Reflect Participation of Several HMGCL Cysteines in Formation of Disulfide Bonds.

Single Cys→Ser substitutions eliminate formation of a covalent intersubunit adduct for nonreduced C266S, C323S, and C170S proteins, suggesting that each of these three residues influences formation of the disulfide linked dimer. Involvement of C323 does not seem surprising, given its reasonable proximity (~14 Å) to C266 located in a flexible and highly conserved “signature” loop of the adjacent HMGCL subunit. Proximity

between this C323-C266 pair of residues is unmatched by any other intersubunit cysteine pair (Figure 2.1C). Given the involvement of C266 in reaction catalysis, tethering the C323-C266 residues together accounts for a diminution in catalytic rate. Coexpression of C266S and C323S proteins to produce a C266S/C323S heterodimeric protein has been essential to generating *experimental* evidence (Figure 2.5) that the proposed C266-C323 adduct can, in fact, explain the formation of a covalent dimer in nonreduced HMGCL.

The role of C170 in influencing covalent adduct formation is less obvious. Given the proximity between C170 and C174 (~4 Å; Figure 2.1B), it is certainly plausible that they could form an intrachain disulfide in nonreduced protein. C266 is more distant (8-10 Å) from these residues. In C170S, given the dynamic nature of the flexible loop that harbors C266, the absence of C170's sulfhydryl may increase the possibility of formation of an intrachain disulfide between C174 and C266 in competition with any interchain C266-C323 dimer adduct (Figure 2.7). In contrast, for C174S good formation of a covalent dimer is observed for nonreduced protein. This suggests that C170 is not as effective as C174 in competing for the intrachain C266, even though both are in reasonable proximity. A structure based HMGCL alignment (63) indicates that C170 is positioned at the end of a beta strand ( $\beta$ 5) while C174 is positioned in the middle of the loop between beta strand 5 and alpha helix 7, which may slightly improve its access to C266.

The double mutant C170S/C174 exhibits strong formation of a covalently linked dimer (Figure 2.6B, lane 3), reversing the elimination of such an adduct that is observed for the single mutant C170S. The hypothesis presented above straightforwardly accommodates this observation. The absence of thiol containing side chains at both

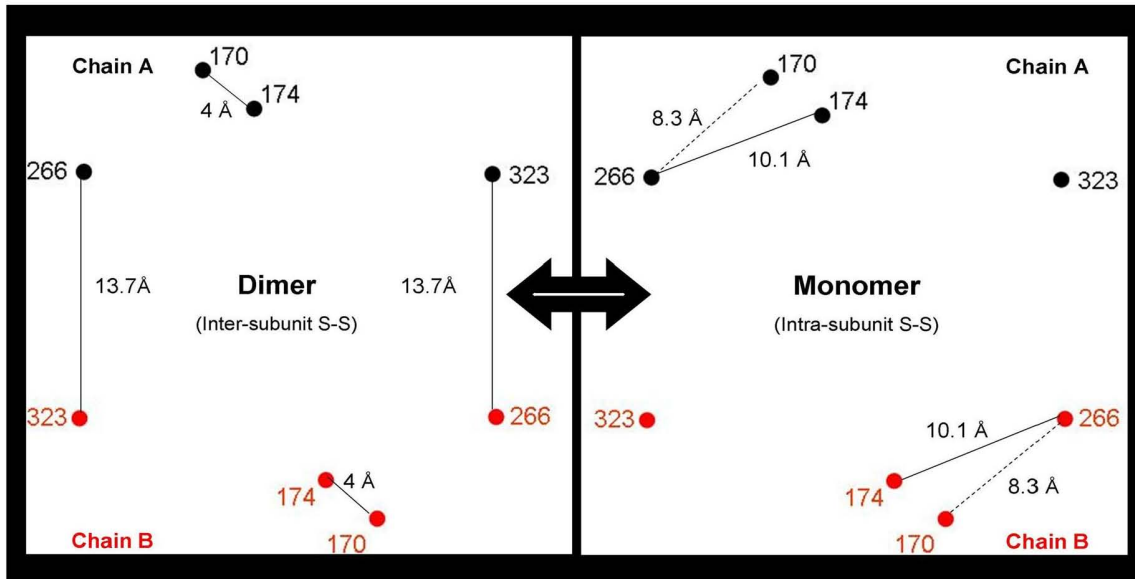


Figure 2.7. Basic model for residues competing in disulfide bond formation. This model illustrates the hypothesis that if C170 and C174 are not disulfide paired, they may compete with C323 for intrachain pairing with C266, disrupting the inter-subunit disulfide. This C170-C174 pair forms a “protective” disulfide that when disrupted allows a “regulatory” disulfide to form with C266. Although C266 is closer to C170 than C174, both the absence of a C170S mutant dimer upon non-reducing SDS-PAGE and the magnitude of the dependence on thiol for C170S activity suggest that a C266-C174 disulfide is more favorable than a C266-C170 disulfide.

residues 170 and 174 eliminates the possibility that *either* residue forms an intrachain disulfide with C266. Thus in nonreduced C170S/C174S, without competition by these residues for C266, an increase in formation of the interchain adduct between C266 and C323 of the adjacent subunit is favored, accounting for the SDS-PAGE detection of a substantial formation of this adduct.

## CHAPTER 3

### DISCOVERY OF AN EXTRAMITOCHONDRIAL HUMAN HMG-COA LYASE

#### **Introduction**

Although glucose is the primary fuel for the brain, the ketone bodies 3-hydroxybutyrate and acetoacetate become important substrates for energy and/or substrate production during conditions such as starvation and development. Hepatocytes are traditionally thought of as supplying extra-hepatic tissues with ketone bodies; however evidence is accumulating that astrocytes are also ketogenic cells. Astrocyte ketogenesis may exert neuroprotective effects both by scavenging non-esterified fatty acids released during brain trauma and ischemia, preventing detrimental effects such as uncoupling of oxidative phosphorylation and by serving as an energy substrate, preserving neuronal function and stability. (64) Ketone bodies have also been shown to protect neurons in models of Alzheimer's and Parkinson's disease and ketogenic diets have been used for many years as an alternative treatment for epilepsy. (65)

Based on sequence homology, the National Institute of Health's Mammalian Gene Collection Program (MGC) has recently identified the protein encoded by the gene 3-hydroxymethyl-3-methylglutaryl-Coenzyme A lyase-like 1 (HMGCLL1) as being a potential HMG-CoA lyase. (66) Human HMG-CoA lyase is found in mitochondria and peroxisomes of most tissues (primarily in liver) however, HMGCLL1 transcripts are found primarily in the brain and heart. The human HMGCLL1 gene maps to chromosome 6p12.1 and spans about 144.7 Kb while the human HMG-CoA lyase gene has been mapped to chromosome 1p36.1-p35 and spans only about 23.6 Kb. Although

HMGCLL1 contains the HMG-CoA lyase signature sequence, the difference in location and structure of the HMGCLL1 gene raises the question: Does the HMGCLL1 gene encode a functional protein or is it a pseudogene? The purpose of this research is to express and purify the HMGCLL1 gene product so that its functional activity, sub-cellular localization, and possible post-translational modifications may be characterized.

## **Materials and Methods**

### Materials

*E. coli* JM109 and BL21 (DE3) competent cells, miniprep, midiprep, and gel purification kits were purchased from Promega. dNTPs and *Pfu* DNA polymerase used for mutagenesis were purchased from Stratagene. Primers used for mutagenesis were synthesized by Integrated DNA Technologies. *EcoRI*, *XhoI*, *NcoI*, *BamHI*, *SacI*, and *DpnI* endonucleases were obtained from New England Biolabs. DNA sequencing was performed at the DNA Core Facility, University of Missouri-Columbia. The Easy Select *Pichia* Expression Kit and Zeocin were purchased from Invitrogen. Glass beads, Fluoro-Hance, and IPTG were purchased from Research Products International. Bradford reagent, chelex-100, and unstained protein standards were purchased from Bio-Rad. Ni-Sepharose was purchased from GE Healthcare, [9,10-<sup>3</sup>H(N)]myristic acid from Perkin Elmer, and autoradiography film from MIDSCI (St. Louis, MO). ECL reagents, PMSF, and peroxidase suppressor were obtained from Pierce. Glycerol, PonceauS, Tween 20, EGTA, deoxycholate, acyl-CoA synthetase, protease inhibitors, NAD, NADH, malic acid, and coupling enzymes were purchased from Sigma-Aldrich. Antibiotics, DNA

ligase, DNase I, media components, buffers, DTT, and all other reagents were obtained from Fisher Scientific.

### Plasmid Construction

The open reading frame encoding full-length HMGCLL1 isoform b was sub-cloned into the expression vectors pPICZ A (Invitrogen) and pET23d (Novagen) using standard molecular biology techniques. The HMGCLL1 coding sequence was amplified from IMAGE Clone ID 4818781 (67) by PCR using primers complimentary to the 5' and 3' ends of the gene. For insertion of the gene into the pPICZ A vector, the 5' primer (5'-**AAAAAAGAATTCATAATGGGGAATGTGCCATCCGCG**-3') encoded an *EcoRI* site (underlined) and a partial yeast Kozak consensus sequence (68) (boldface) which includes the ATG start codon; the 3' primer (5'-**AAAAAACTCGAGTCAATGATGATGATGATGATGAGCATTGAAGG**-3') encoded six histidines (boldface) followed by a stop codon (italicized) and finally an *XhoI* site (underlined). A G2A HMGCLL1 mutant was also constructed to preclude myristoylation by amplifying the gene using a 5' primer (5'-**AAAAAAGAATTCATAATGGCGAATGTGCCATCCGCG**-3') which encoded an *EcoRI* site (underlined), a partial yeast Kozak consensus sequence (68) (boldface) including the ATG start codon, and the single base substitution G5C (italicized), coding for an alanine at position 2 instead of glycine. For insertion of the gene into the pET28d vector, the 5' primer (5'-**GCCGCCACAGGCTCCGCCA**-3') encoded a partial *NcoI* site (underlined); the 3' primer (5'-**AAAAAAGGATCCTCAATGATGATGATGATGATGAGCATTGAAGG**-3')

encoded six histidines (boldface) followed by a stop codon (italicized) and finally an *BamHI* site (underlined). The amplified DNA was digested with the restriction endonucleases *EcoRI* and *XhoI* or *NcoI* and *BamHI* and gel purified. The purified restriction fragment was ligated with a similarly digested and purified pPICZ A or pET28d vector respectively. The ligations produced the constructs pPICZ-HLL1-His<sub>6</sub>, pPICZ-HLL1-G2A-His<sub>6</sub>, pET28-HLL1, and pET28-HLL1-His<sub>6</sub> which encode full-length HMGCLL1 with or without a C-terminal His<sub>6</sub> tag. DNA sequence analysis was used to verify the integrity of the final products.

#### Mutagenesis

A pET28-HLL1-G2A-His<sub>6</sub> mutant was generated using full circle PCR according to Stratagene's QuickChange site-directed mutagenesis protocol. The WT pET28-HLL1-His<sub>6</sub> construct was used as a template. The mutation was verified by DNA sequence analysis. Forward and reverse mutagenic primer sequences (mutagenic bases underlined) are as follows:

CLL1-G2A-F: 5'-GGAGATATAACCATGGGCGAATGTGCCATCCGCG-3'

CLL1-G2A-R: 5'-CGCGGATGGCACATTCGCCATGGTATATCTCC -3'

#### Expression of HMGCLL1 in Inclusion Bodies

Chemically competent *E. coli* BL21 (DE3) cells were transformed with pET28-HLL1-His<sub>6</sub> or pET28-HLL1-G2A-His<sub>6</sub> plasmids, plated onto LB agar containing 100 µg/ml amp, and incubated overnight at 37°C. A single colony was used to inoculate a small volume of LB/amp for overnight growth. Glycerol stocks were made from the overnight culture by combining 1 ml of culture with 0.5 ml of sterile 50% (v/v) glycerol

and storing at  $-80^{\circ}\text{C}$ . A 50 ml starter culture of LB/amp was inoculated from glycerol stock, incubated overnight at  $37^{\circ}\text{C}$ , and 2-3 ml used to inoculate a 1 L culture of LB/amp. After incubation at  $37^{\circ}\text{C}$  until the  $\text{OD}_{600}$  was 0.6 – 0.8, protein expression was induced by the addition of sterile IPTG to a final concentration of 1 mM. After overnight incubation at  $37^{\circ}\text{C}$ , the induced cells were harvested by centrifugation and pellets were stored at  $-80^{\circ}\text{C}$  until protein purification.

#### Purification of HMGCLL1 from Inclusion Bodies

Bacterial cell pellets from 1 L of culture were resuspended in 50 ml of ice cold lysis buffer containing 50 mM tris (pH 8.0), 1 mM EDTA, and 25% (w/v) sucrose. Immediately before cell disruption, 1 mM PMSF, 1 U/ml DNaseI, and 5 mM mercaptoethanol were added. Cells were mechanically disrupted by passing twice through a microfluidizer at  $\sim 17$  kpsi. The lysate was centrifuged at  $17,400 \times g$  for 20 min. at  $4^{\circ}\text{C}$  to collect inclusion bodies. The remaining steps were carried out at room temperature. The pellet was resuspended by homogenization ( $\sim 5$  strokes) in 40 ml of wash buffer containing 20 mM tris (pH 8.0), 200 mM NaCl, 1% (w/v) Na deoxycholate, and 2 mM EGTA. The suspension was centrifuged and the pellet resuspended as above three times in 40 ml of wash buffer containing 10 mM tris (pH 8.0), 0.25% (w/v) Na deoxycholate, and 1 mM EGTA. The final pellet was resuspended by homogenization ( $\sim 10$  strokes) in buffer containing 10 mM tris (pH 8.0), 8 M urea (or 6 M GdHCl). The suspension was diluted to 6 M urea, centrifuged as above, and the supernatant was stored at room temperature until use. Protein concentration was determined by the method of Bradford (69). A typical expression and purification yields about 100 mg of protein.

## Antibody Production and Purification

A synthetic peptide corresponding to residues 19-37 of human HMGCLL1 (a region which is not conserved in mitochondrial HMG-CoA lyase; Figure 3.1) was produced, conjugated to KLH, and used to raise antibodies in rabbits by Global Peptide Services (Fort Collins, CO). For immunofluorescence microscopy, antibodies were purified essentially as described by Pringle *et al.* (70). Briefly, protein purified from inclusion bodies (described above) was further purified by application to a 2 ml Ni-sepharose column equilibrated in 10 mM tris (pH 8.0), 6 M urea. The column was washed overnight with a 525 ml gradient of 6 to 0 M urea, 25 mM tris (pH 8.0), 5 mM mercaptoethanol, 1 mM L-arginine, 1 mM MgCl<sub>2</sub>, 150 mM NaCl, 20% (v/v) glycerol, and 0.05% (v/v) TX-100. The protein was eluted slowly overnight with 25 mM tris (pH 8.0), 5 mM metcaptoethanol, 200 mM NaCl, 300 mM imidazole, 20% (v/v) glycerol, and 0.05% (v/v) TX-100. A 12% SDS gel was prepared using a 2-D electrophoresis comb to produce a single 6.7 mm wide well. Sixty-seven micrograms of purified HMGCLL1 was loaded evenly across the well and the sample was run for 10 min at 110 V. This was repeated five more times to produce a total of 6 strips of protein. Following the last load, the gel was allowed to run until the dye front was ~ 1 cm from the bottom of the gel and the protein was transblotted to nitrocellulose overnight. The blot was stained with PonceauS, the protein strips were cut out, destained with TBS, and stored dry until use. Following blocking with non-fat milk, 100 – 200 µl of crude, non-diluted anti-serum was laid on each strip and incubated for 2 hrs at RT, with agitation. The depleted anti-serum was removed, frozen, and re-used for subsequent purifications until the yield became

poor. The protein strips with bound antibody were washed 3 times in TBS, the antibodies were eluted with 0.2 M glycine (pH 2.5), 1 mM EGTA (~ 100  $\mu$ l per strip), and eluted antibodies were immediately neutralized with 1M tris (pH 8.0). The protein strips were neutralized with several washes in TBS, air-dried, and stored for subsequent purifications. The purified antibodies were buffer exchanged into PBS with 0.1% (w/v) BSA by centrifugal ultrafiltration to a final antibody concentration of about 1 mg/ml (as determined by  $A_{280}$ ;  $\epsilon_{1\%} = 13.5$ ) and stored in aliquots at  $-80^{\circ}\text{C}$  until use.

### Native Protein Expression

Chemically competent *Pichia pastoris* KM71H cells were prepared using an Invitrogen EasyComp Transformation kit. pPICZ-HLL1-His<sub>6</sub> and pPICZ-HLL1-G2A-His<sub>6</sub> plasmids were propagated in *E. coli* JM109 cells and purified from 50 ml of LB + 25  $\mu$ g/ml Zeocin using a Qiagen midi prep kit, yielding 150 – 200  $\mu$ g of each plasmid. Purified plasmids were linearized by digestion with *SacI* endonuclease and 3  $\mu$ g of each were transformed into *P. pastoris* KM71H cells as per the EasyComp (Invitrogen) protocol. Transformation reactions were plated on yeast extract peptone dextrose (YPD) + 100  $\mu$ g/ml Zeocin and incubated at  $30^{\circ}\text{C}$  until colonies formed (3-5 days). Integration of *hmgc11* was confirmed by direct PCR screening (71) using the primers described for plasmid construction. An isolated colony of each integrant was used to inoculate 4 ml of YPD for overnight growth. A glycerol stock of each confirmed integrant was made by combining 1 ml of culture with 0.5 ml of sterile 50% (v/v) glycerol and storing at  $-80^{\circ}\text{C}$ . Small-scale cultures were then analyzed by Western blot to select an integrant with good HMGCLL1 expression. For full-scale expression, a 75 ml starter culture of minimal

glycerol + histidine media (MGYH) was inoculated from glycerol stock and incubated at 25°C with vigorous shaking until the OD<sub>600</sub> was about 5 (late log phase). Ten milliliters of the starter culture was used to inoculate each of three 1 L cultures of MGYH which were incubated as above until the OD<sub>600</sub> was about 6. Expression of HMGCLL1 was induced by harvesting the cells by centrifugation at 3,000 xg for 5 min at RT in a sterile centrifuge tube and resuspending the pellets in 750 ml of minimal methanol + histidine media (MMH). Induced cultures were incubated at 25°C with vigorous shaking and induction was maintained by the addition of 3.75 ml of 100% methanol every 24 hrs. At 72 hrs post-induction, cells were harvested by centrifugation at 5,000 xg for 6 min at RT and pellets (~20 g of wet cells) were stored at -80°C until protein purification. Similar conditions were used for expression of the HLL1-G2A-His<sub>6</sub> mutant.

#### Native Enzyme Purification

All steps were carried out at 4°C. Bacterial pellets from 750 ml of induction culture were resuspended in 400 ml of ice cold lysis buffer containing 25 mM NaP<sub>i</sub> (pH 7.4), 300 mM NaCl, 10% (v/v) glycerol, 1% (v/v) Triton X-100, and 10 mM imidazole. Protease inhibitors (1 mM PMSF, 1 μM pepstatinA, and 10 μM leupeptin), and 5mM mercaptoethanol were added immediately before cell disruption. The cell suspension was split in half and cells were mechanically disrupted in a Bead Beater (Bio Spec) half full of ice cold glass beads (0.5 mm) for 12 cycles of 30 sec with a 60 sec pause between each cycle. The glass beads were separated from the lysate using a large, empty chromatography column and both batches of lysate were combined. DNase I was added to the lysate at a final concentration of 1 U/ml and incubated for 15 min. at 4°C. A gram

of Chelex-100 was added to the lysate just prior to clarification by centrifugation at 3,000 xg (wt HMGCLL1) or 5,000 xg (G2A HMGCLL1) and the supernatant was loaded onto Ni-Sepharose Fast Flow resin (0.2 – 0.4 ml). The column was washed with 25 mM NaP<sub>i</sub> (pH 7.4), 250 mM NaCl, 10% (v/v) glycerol, 0.1% (v/v) Triton X-100, 50 mM imidazole, and 5 mM mercaptoethanol until the A<sub>280</sub> < 0.010. The protein was eluted slowly overnight with 25 mM NaP<sub>i</sub> (pH 7.4), 250 mM NaCl, 10% (v/v) glycerol, 0.1% (v/v) Triton X-100, 300 mM imidazole, and 5 mM mercaptoethanol. Fractions containing HMGCLL1 were pooled, concentrated by centrifugal ultrafiltration, and the final concentration was determined by the method of Bradford (72). Similar conditions were utilized for the purification of the G2A mutant. A typical expression and purification yielded 0.1 to 0.5 mg of wt or G2A HMGCLL1.

#### Enzyme Activity Measurement

Enzyme activity was determined using the method of Stegink and Coon (73) as modified by Kramer and Miziorko (74). HMG-CoA was synthesized using the method of Goldfarb and Pitot (75). Briefly, this spectrophotometric assay couples the acetyl-CoA produced upon the cleavage of HMG-CoA to the reactions of malate dehydrogenase and citrate synthase. For each acetyl-CoA that condenses with oxaloacetate to form citrate, one malate is oxidized to oxaloacetate, producing one NADH. The rate of NADH production is determined by measuring the increase in A<sub>340</sub> and is proportional to the amount of HMG-CoA lyase added. For estimates of maximum velocity (V<sub>max</sub>) and Michaelis constant (K<sub>m</sub>), reaction velocities at varying substrate concentrations were fitted to the Michaelis-Menten equation using GraphPad Prism 4.0 (GraphPad Software,

San Diego, CA). For determination of the  $K_m$  for  $Mg^{2+}$  and  $Mn^{2+}$ , all assay components including buffers and enzymes were treated with Chelex-100 to remove trace metals. Assays for estimates of maximum velocity ( $V_{max}$ ) and Michaelis constant ( $K_m$ ) contained 3 nM HMGCLL1 or G2A HMGCLL1.

#### Expression and Purification of Human N-myristoyltransferase

The pET15-MHL vector containing the gene for human NMT1 was obtained from Structural Genomics Consortium (Toronto, Canada; deposited by Cheryl Arrowsmith) harbored in *E. coli* DH5 $\alpha$  cells. The plasmid was purified and transformed into chemically competent *E. coli* BL21 (DE3). Transformed cells were plated onto LB agar containing 100  $\mu$ g/ml amp, and incubated overnight at 37°C. A single colony was used to inoculate a small volume of LB/amp for overnight growth. Two milliliters of the overnight culture was used to inoculate a 1 L culture of LB/amp. The culture was incubated at 37°C until the OD<sub>600</sub> was 0.6 – 0.8 at which point protein expression was induced by the addition of sterile IPTG to a final concentration of 1 mM and the temperature was reduced to 20°C. After overnight incubation the induced cells were harvested by centrifugation, the pellet was resuspended in 40 ml of cold lysis buffer (50 mM HEPES (pH 7.5), 500 mM NaCl, 5 mM imidazole, 5% (v/v) glycerol, 2.5 mM PMSF, and 10  $\mu$ M pepstatin), and the suspension was stored at -80°C until protein purification. All purification steps were carried out at 4°C. The cell suspension was thawed, the volume adjusted to 100 ml with lysis buffer, and 1 U/ml DNaseI was added. Cells were mechanically disrupted by passing twice through a microfluidizer at ~17 kpsi. The lysate was clarified by centrifugation at 20,000 xg for 1 hr and the supernatant was

loaded onto Ni-Sepharose Fast Flow resin (~0.5 ml). The column was washed with 50 mM HEPES (pH 7.5), 500 mM NaCl, 30 mM imidazole, and 10% (v/v) glycerol until the  $A_{280} \sim 0.075$ . The protein was eluted slowly overnight with 50 mM HEPES (pH 7.5), 500 mM NaCl, 250 mM imidazole, and 20% (v/v) glycerol. Fractions containing NMT were pooled and the concentration was determined by the method of Bradford (76). About 7 mg of homogeneous enzyme was produced.

#### In-vitro N-myristoylation Assay

First, [ $^3\text{H}$ ]myristoyl-CoA was synthesized by adding 0.03 U of *Pseudomonas* sp. acyl-coenzyme A synthase to 100  $\mu\text{l}$  of buffer (20 mM Tris (pH 7.4), 1 mM DTT, 10 mM  $\text{MgCl}_2$  0.1 mM EGTA) containing 6 mM coenzyme A, 12 mM ATP, and 3.3  $\mu\text{M}$  [9,10- $^3\text{H}(\text{N})$ ]myristic acid (30 Ci/mmol). The reaction was incubated at 37°C for 2 hrs. with agitation. Then, the NMT reaction was initiated by addition of 10  $\mu\text{l}$  synthesized [ $^3\text{H}$ ]myristoyl-CoA to 10  $\mu\text{l}$  of NMT reaction mixture containing 1 mM EDTA, 0.2% TX-100, 7.4  $\mu\text{g}$  HMGCLL1 purified from inclusion bodies, and 6.2  $\mu\text{g}$  of purified human NMT. This reaction was incubated overnight at 25°C. The protein precipitate that formed was collected by desktop centrifugation for 5 min and the pellet dissolved in SDS loading buffer. Finally, the resuspended precipitates were run on a 12% SDS gel, the gel soaked in Fluoro-Hance, dried, and exposed to autoradiography film for 3 days at -80°C.

#### Immunofluorescence in COS-I cells

Full-length *hmgcll1* and G2A *hmgcll1* were sub-cloned into the expression vector pcDNA3 (Invitrogen) using standard molecular biology techniques. Briefly, the gene was amplified from PICZ-HLL1-His<sub>6</sub> using the primers described in Plasmid

Construction. The PCR products were digested with *EcoRI* and *XhoI*, gel purified, and ligated with a similarly digested and purified pcDNA3 vector backbone. DNA sequence analysis was used to verify the integrity of the pcDNA3-HLL1-His<sub>6</sub> and pcDNA3- HLL1-G2A-His<sub>6</sub> products. COS-1 (American Type Culture Collection) cells were transfected by electroporation with pcDNA3-HLL1-His<sub>6</sub> and pcDNA3- HLL1-G2A-His<sub>6</sub> and cultured to about 80% confluence at 37°C in Dulbecco's modified Eagle's medium (Invitrogen) supplemented with penicillin/streptomycin and 10% (v/v) fetal bovine serum (Invitrogen) in a 5% CO<sub>2</sub> atmosphere. Coverslips were removed from medium and washed 3 times in Dulbecco's phosphate-buffered saline (D-PBS). Cells were then fixed in 3% (w/v) formaldehyde in PBS for 20 min and rinsed 3 times with PBS. Fixed cells were permeabilized with 1% (v/v) TX-100 in PBS for 5 min and rinsed 3 times in PBS. Cells were incubated for 45 min with rabbit anti-HMGCLL1, rinsed 7 times with PBS and then incubated for 45 min with Alexa Fluor 488 labeled goat anti-rabbit IgG. The coverslips were rinsed 7 times with PBS, mounted in 100 mM tris (pH 8.7), 1 mg/ml phenylene diamine. Cells were photographed using a digital camera at 1 – 10 sec.exposures with fluorescent light of appropriate wavelengths.

#### Rat Organ Lysate Blots

Six freshly euthanized 60 day old white rats (3 male, 3 female) were purchased from a local supplier and kept on ice until dissection. The major organs were harvested and homogenized on ice in 3 volumes of homogenization buffer (25 mM HEPES (pH 7.4), 5 mM EDTA, 1 mM DTT, and 0.1% (v/v) Triton X-100). PMSF and pepstatin (1 mM and 1 µM respectively) were added immediately prior to homogenization for 3 cycles of 1

min on, 1 min pause using a Polytron (Brinkman/Kinematica) set on speed 3. Homogenates were clarified by centrifugation at 800 xg for 10 min at 25°C and the supernatants filtered through a 0.2 µm centrifugal device. Ten mg of protein (1-6 µl) from each filtrate was diluted to 100 µl in homogenization buffer without Triton X-100 and applied to nitrocellulose using a Hybri-Slot manifold (Gibco BRL). Casein blocked, peroxidase suppressed blots were incubated separately in 5.6 µg/ml affinity purified anti-HMGCLL1 or anti-HMG-CoA lyase antibodies. Rinsed blots were incubated in a 1:5000 dilution of goat anti-rabbit IgG-horseradish peroxidase conjugated antibodies. Finally, rinsed blots were incubated in West Pico ECL Western Blotting substrate and exposed to autoradiography film.

#### Immunofluorescence in Neuro2a and U87 Cells

U87 cells were grown to about 80% confluence at 37°C in Eagle's minimal essential medium (Invitrogen) supplemented with 10% (v/v) fetal bovine serum, 0.15% (w/v) sodium bicarbonate, 1 mM sodium pyruvate, 0.1 M nonessential amino acids, and 500 µg/mL penicillin-streptomycin in a 5% CO<sub>2</sub> atmosphere. Neuro2a cells (American Type Culture Collection) were grown to about 80% confluence at 37°C in Dulbecco's modified Eagle medium (Invitrogen) supplemented with 10% (v/v) fetal bovine serum and 500 µg/mL penicillin-streptomycin in a 5% CO<sub>2</sub> atmosphere. Coverslips were removed from medium and cells were washed, fixed, and permeabilized as described above. Cells were incubated for 45 min with two primary antibodies, one against a subcellular compartment specific protein and one against either HMGCL or HMGCLL1. For lipid droplet staining, cells were incubated with BODIPY 493/503 and anti-HMGCLL1. Following

incubation with primary antibodies, cells were rinsed 7 times with PBS and then incubated for 45 min with the appropriate fluorescently labeled secondary antibodies. The coverslips were rinsed 7 times with PBS, mounted in 100 mM tris (pH 8.7), 1 mg/ml phenylene diamine. Cells were photographed using a digital camera at 1 – 10 sec.exposures with fluorescent light of appropriate wavelengths. Antibodies (diluted in PBS containing 0.1% (w/v) BSA) are as follows:

1° antibodies-

Affinity purified rabbit anti-HMGCL 1:100 dilution

Affinity purified rabbit anti-HMGCLL1 1:100 dilution

Monoclonal mouse anti-ATP synthase  $\beta$  subunit 1:200 dilution (Sigma)

Sheep anti-catalase 1:100 dilution

2° antibodies-

Cy3 labeled goat anti-rabbit 1:200 dilution

Alexa Fluor 488 labeled goat anti-mouse 1:200 dilution

Alexa Fluor 488 labeled goat anti-rabbit 1:200 dilution

Rhodamine labeled donkey anti-sheep 1:50 dilution

## **Results**

### Comparison of Human HMGCL and Human HMGCLL1

#### Amino Acid Sequences

The HMGCLL1 gene product is a 340 residue protein that is 64% identical and 78% similar to HMG-CoA lyase (Figure 3.1). HMGCLL1 contains the highly conserved HMG-CoA lyase signature sequence GL/AGGCPY/F (residues 277-283; Figure 3.1)

```

          10          20          30          40          50          60
Lyase_human  MAAMRKALPR RLVGLASLR-----AVSTSS MGTLPKRVKI VEVGPRDGLQ
HMGCLL1      MGNVPSAVKH CLSYQQLKRE HLWIGDSVAG ALDPAQTSQ LSGLPEFVKI VEVGPRDGLQ

          70          80          90          100         110         120
Lyase_human  NEKNIVSTPV KIKLIDMLSE AGLSVIETTS FVSPKWVPQM GDHTEVLKGI QKFPGINYPV
HMGCLL1      NEKVIVPTDI KIEFINRLSQ TGLSVIEVTS FVSSRWVPQM ADHTEVMKGI HQYPGVRYPV

          130         140         150         160         170         180
Lyase_human  LTPNLKGFEA AVAAGAKEV IFGAASELFT KKNINCSIEE SFQRFDAILK AAQSANISVR
HMGCLL1      LTPNLQGFHH AVAAGATEIS VFGAASESFS KKNINCSIEE SMCKFEVVVK SARHMNI PAR

          190         200         210         220         230         240
Lyase_human  GYVSCALGCP YEGKISPAKV AEVTKKFSM GCYEISLGDY IGVGTPGIMK DMLSAVMQEV
HMGCLL1      GYVSCALGCP YEGSITPQKV TEVSKRLYGM GCYEISLGDY IGVGTPGSMK RMLSEVMKEI

          250         260         270         280         290         300
Lyase_human  PLAALAVHCH DTYGQALANT LMALQMGVSV VDSSVAGLGG CPYAQGASGN LATEDLVYML
HMGCLL1      PPGALAVHCH DTYGQALANI LTALQMGINV VDSAVSGLGG CPYAKGASGN VATEDLIYML

          310         320         330         340
Lyase_human  EGLGIHTGVN LOKLLEAGNF ICQALNRRTS SKVAQATCKL
HMGCLL1      NGLGLNTGVN LYKVMEAGDF ICKAVNKITN SKVAQASFNA

```

Figure 3.1. A sequence alignment comparing the sequences of HMG-CoA lyase and HMGCLL1 from *Homo sapiens* (human). Identical residues are in bold. A dashed underline indicates a mitochondrial leader sequence. A solid underline denotes residues consistent with an N-myristoylation motif. Boxed residues represent the HMG-CoA lyase signature sequence. Residues corresponding to the anti-HMGCLL1 antibody epitope are circled.

which is found in all HMG-CoA lyase proteins identified to date. HMGCLL1 lacks the N-terminal mitochondrial leader sequence found in HMGCL and instead features an N-myristoylation motif. N-myristoyltransferase absolutely requires a terminal glycine (following methionine cleavage by methionine aminopeptidase) followed by an uncharged residue. Residues three and four may be any residue. The fifth residue is a small uncharged residue but serine is favored. The sixth residue may not be proline (77). Although HMGCLL1's N-terminus is not conserved in HMGCL, it is well conserved among higher vertebrate HMGCLL1 sequences (Figure 3.2). At the C-terminus, HMGCLL1 lacks the peroxisomal targeting sequence CK/RL present in HMGCL. Mammalian HMG-CoA lyases contain 8 highly conserved cysteines. Interestingly, although HMGCLL1 also contains 8 cysteines it lacks the C-terminal cysteine implicated in regulation by thiol/disulfide exchange (78, 79, 80). Instead, the 8<sup>th</sup> cysteine in HMGCLL1 is located in its non-conserved leader sequence. These sequence features suggest that HMGCLL1 may be an active, extramitochondrial HMG-CoA lyase that is N-terminally modified with myristic acid.

#### Specificity of Anti-HMGCLL1 Antibody

The calculated monomer molecular mass for HMGCLL1, full-length HMGCL, and mature HMGCL are relatively close at 36,300 Da, 34,400 Da, and 31,600 Da respectively. To aid in identification of HMGCLL1 in complex samples and to distinguish it from mitochondrial and peroxosomal HMGCL, an antibody was raised in rabbit against a synthetic peptide corresponding to residues 19-37 of the non-conserved HMGCLL1 N-terminus (Figure 3.1). When used to probe Western blots of purified

	10	20	30	40
	..... .....	..... .....	..... .....	..... .....
hHMGCL	<b>MAAMRKALPR</b>	<b>RLVGLASLRA</b>	<b>VS</b> -----	-----
Human	<b>MGNVPSAVKH</b>	<b>CLSYQ-QLLR</b>	<b>EHLWIGDSVA</b>	<b>GALDPAQ---</b>
Rhesus monkey	<b>MGNVPSAVKH</b>	<b>CLSYQ-QLLR</b>	<b>EHLWIGDSVA</b>	<b>GALDPAQISV</b>
Canine	<b>MGNVPSAVKH</b>	<b>CLSYQ-QLLR</b>	<b>EHLWIGDSVA</b>	<b>GALDTAQ---</b>
Bovine	<b>MGNVPCAVKH</b>	<b>CLSYQ-QLLR</b>	<b>EHLWIGDSVA</b>	<b>GALEPAQ---</b>
Rat	<b>MGNLPSAAKH</b>	<b>CLNYQ-QLLR</b>	<b>EHLWSGESVA</b>	<b>GALDPAQ---</b>
Mouse	<b>MGNLPSAAKH</b>	<b>CLNYQ-QLLR</b>	<b>EHLWSGDSVA</b>	<b>GALDAAQ---</b>
Opossum	<b>MGNMPSAVKH</b>	<b>CLSYQ-HLLR</b>	<b>EHLGVGDPVA</b>	<b>GALEPAQ---</b>
Horse	<b>MGNVPSRSEA</b>	<b>LPSATNSFLR</b>	<b>KHLWIGDSVA</b>	<b>GAPDPAQ---</b>
Red Jungle Fowl	<b>MGTVP SALKH</b>	<b>CLSYQ-HLLK</b>	<b>EQLWIGEPTA</b>	<b>-PPHPGQ---</b>
Zebrafish	<b>MGNVSSAVKH</b>	<b>CLSYE-TFLR</b>	<b>DYPWLP----</b>	<b>RLLWEEK---</b>

Figure 3.2. A sequence alignment comparing the N-terminal sequences of human HMG-CoA lyase and HMGCLL1 from a variety of vertebrates. Identical residues are in bold.

HMGCLL1, HMGCL, and *B. subtilis* proteins, the anti-HMGCLL1 antibody detects only the HMGCLL1 protein (Figure 3.3A). In contrast, the anti-avian HMGCL antibody detects all three proteins (Figure 3.3B). When used to probe Western blots of *E. coli* and *P. pastoris* whole cell lysates expressing HMGCLL1, the anti-HMGCLL1 antibody detects only a single band at the molecular mass expected for HMGCLL1 protein (Figure 3.4).

### Expression and Purification of HMGCLL1

Initially, HMGCLL1 was cloned into a variety of vectors including pET and pTrc for expression in *E. coli*. Expression trials were performed at varying temperatures, IPTG concentrations, and induction periods using BL21 (DE3), Arctic Express, and C43 strains of *E. coli*. Although HMGCLL1 was expressed as a large fraction of the total *E. coli* lysate, most of the target protein was recovered in the insoluble fraction even under optimized conditions. Since several *E. coli* expression systems failed to produce milligram quantities of purified, intact protein from a reasonable culture volume, the methylotrophic yeast *Pichia pastoris* was chosen as the expression system. Although HMGCLL1 was expressed as only a small fraction of the total *P. pastoris* lysate, about 0.5 mg of > 95% homogenous protein was purified by immobilized metal affinity chromatography (IMAC) from 750 ml of induction culture (Figure 3.5). During initial attempts at purification it was observed that upon high-speed centrifugation, lyase activity could be found in the pellet fraction. The addition of triton X-100 to purification buffers and minimizing centrifugation of the crude lysate improved the yield of protein in the supernatant. The nickel-column eluate remains in the supernatant fraction even upon

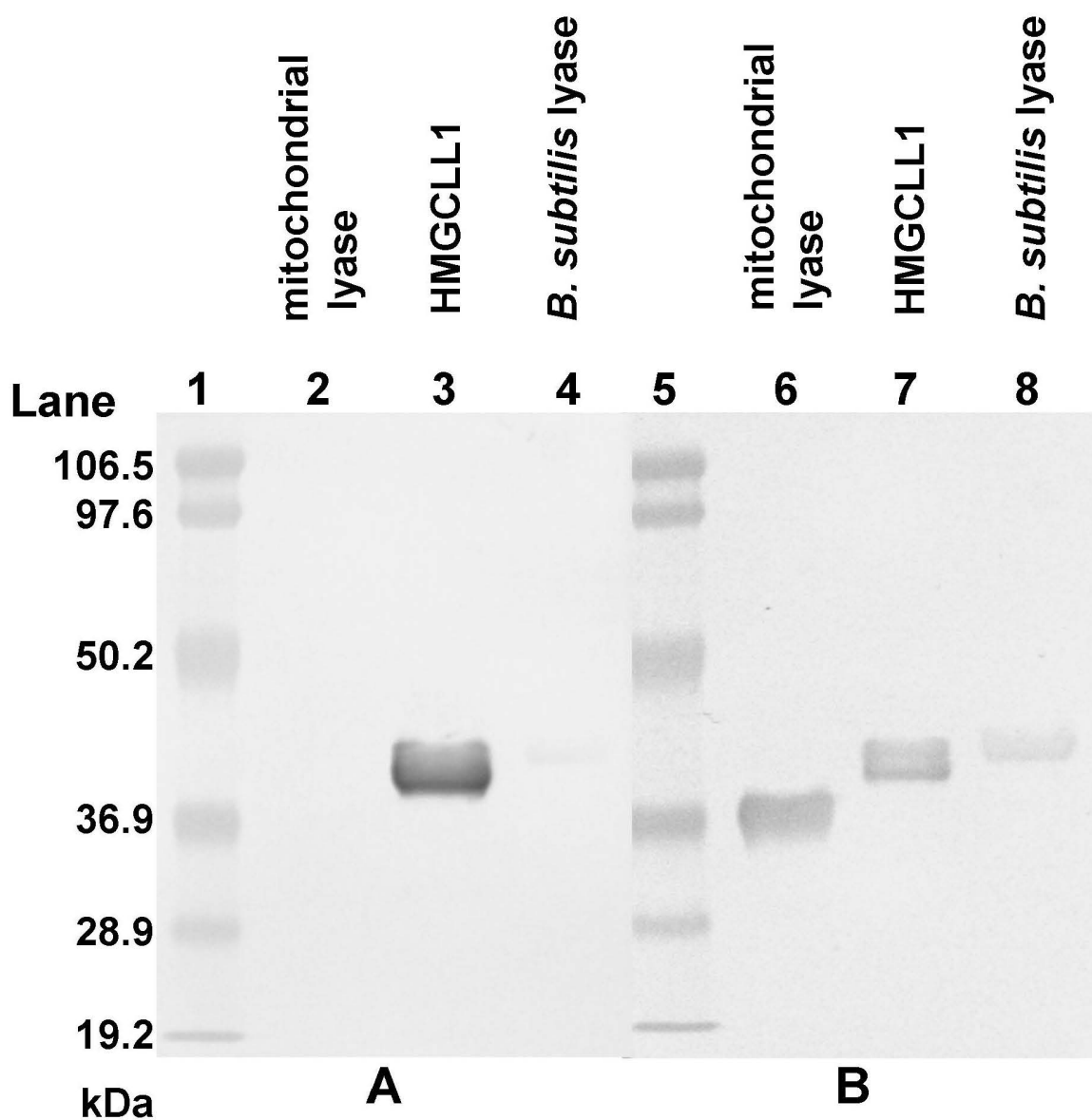


Figure 3.3. Specificity of anti-HMGCLL1 antibody. Human mitochondrial HMG-CoA lyase, wild-type HMGCLL1, and *B. subtilis* HMG-CoA lyase (purified, 1  $\mu$ g each) were run in duplicate on an SDS gel and transblotted to nitrocellulose. The duplicate halves were separated and treated individually with either rabbit anti-HMGCLL1 antibody (whole serum) [A] or rabbit anti-avian HMG-CoA lyase antibody (whole serum) [B]. The blots were incubated with alkaline phosphatase conjugated secondary antibody and developed colorimetrically using 5-bromo-4-chloro-3-indolyl-phosphate (BCIP)/ nitro blue tetrazolium (NBT). Prestained molecular weight markers include: phosphorylase b, 105.5 kDa; bovine serum albumin, 97.6 kDa; ovalbumin, 50.2 kDa; carbonic anhydrase, 36.9 kDa; trypsin inhibitor, 28.8 kDa; lysozyme, 19.2 kDa.

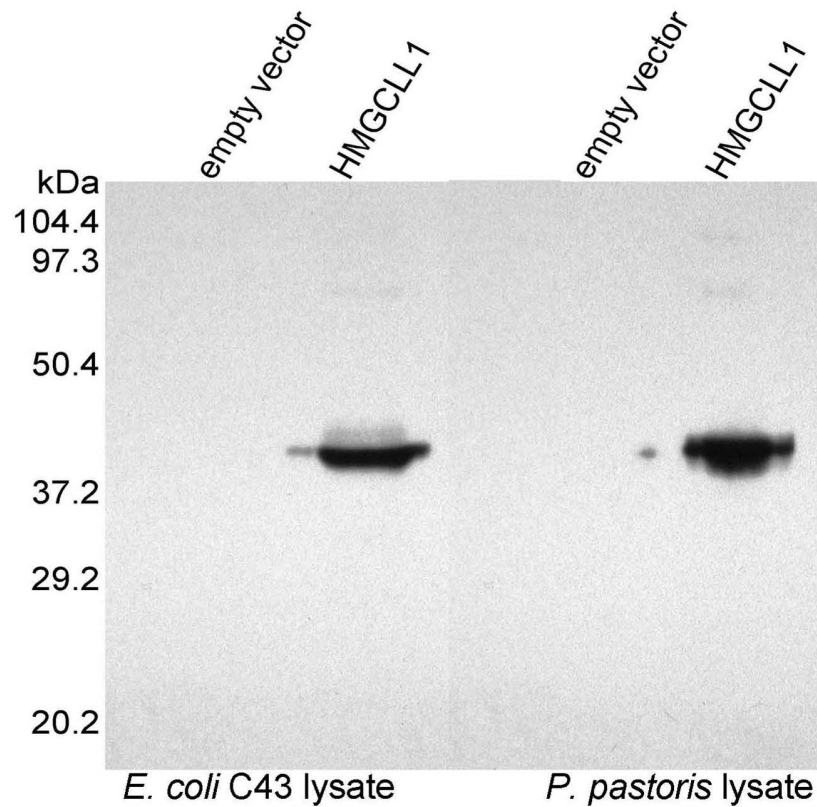


Figure 3.4. The anti-HMGCLL1 antibody does not react with endogenous *E. coli* or *P. pastoris* proteins. Crude lysates (10  $\mu$ g each) of *E. coli* C43 and *P. pastoris* cells expressing HMGCLL1 or transformed with empty vectors were run on an SDS gel and transblotted to nitrocellulose. The blot was incubated with affinity purified rabbit anti-HMGCLL1 antibody, horseradish peroxidase conjugated secondary antibody, and developed by enhanced chemiluminescence. Prestained molecular weight markers include: phosphorylase b, 104.4 kDa; bovine serum albumin, 97.3 kDa; ovalbumin, 50.4 kDa; carbonic anhydrase, 37.2 kDa; trypsin inhibitor, 29.2 kDa; lysozyme, 20.2 kDa. Positions indicated for pre-stained molecular weight standards are determined when exposed autoradiography film is overlaid on the western blot.

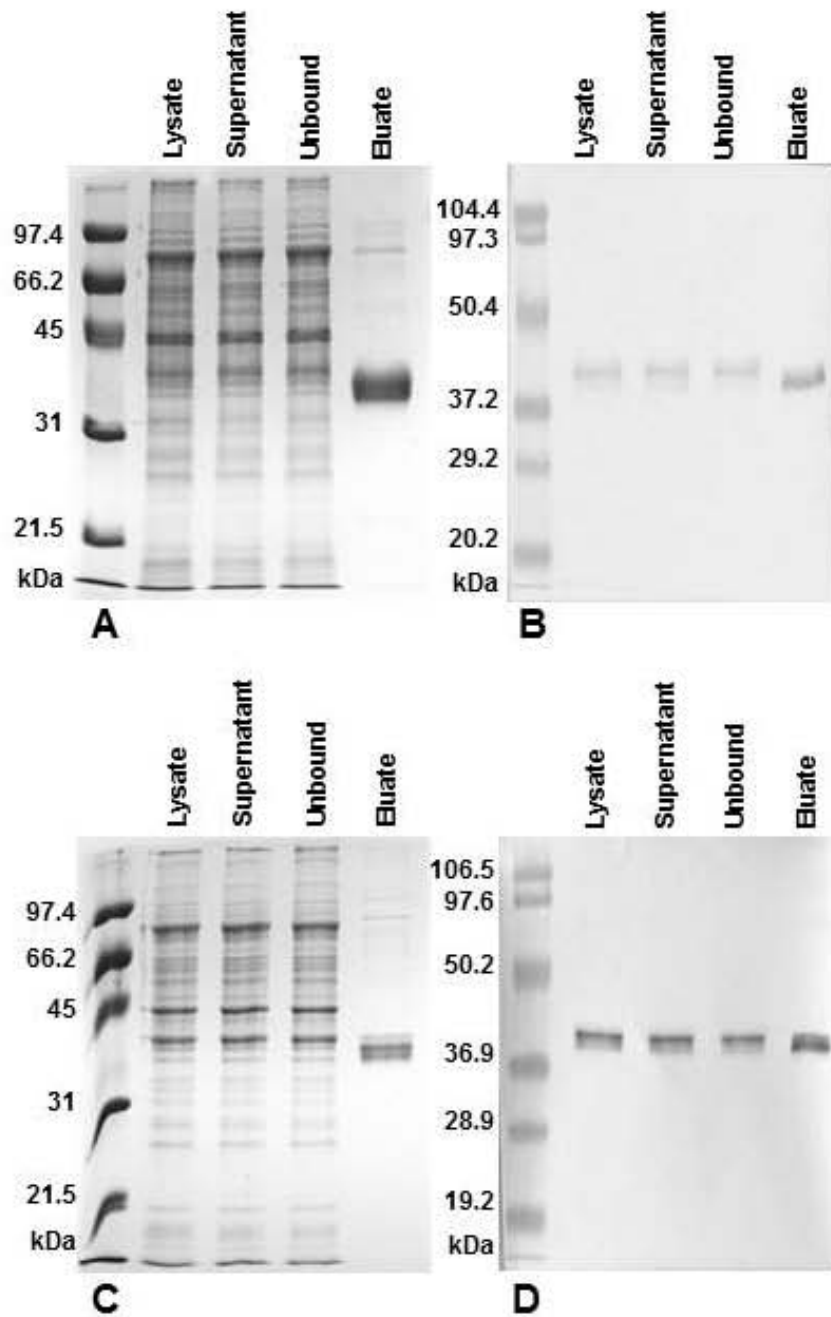


Figure 3.5. SDS gels (A, C) and Western blots (B, D) of fractions from the purification of wild-type (A, B) and G2A (C, D) HMGCLL1. Ten micrograms of each lysate, supernatant, and unbound fraction as well as 5 ug (1 ug for Western) of Ni-sepharose eluate were run in duplicate on a 10% SDS gel. One half of the gel was Coomassie stained while proteins on the other half were transblotted to nitrocellulose. The blots were incubated with rabbit anti-HMGCLL1 antibody (whole serum). The blots were incubated with goat anti-rabbit IgG alkaline phosphatase conjugated secondary antibody and developed colorimetrically using 5-bromo-4-chloro-3-indolyl-phosphate (BCIP)/ nitro blue tetrazolium (NBT). Molecular weight markers include (highest to lowest): phosphorylase b, bovine serum albumin, ovalbumin, carbonic anhydrase, trypsin inhibitor, and lysozyme.

extended high-speed centrifugation. Although a variety of protease inhibitors are present during purification, the protein is often observed as a doublet when denatured protein is examined by SDS-PAGE (Figure 3.6). Edman sequencing revealed that discrete cleavage occurs after residue 17 (leucine) in *E. coli* preparations and after residue 18 (leucine) in *P. pastoris* preparations (Table 3.2). The susceptibility of this site to proteolysis suggests that this region of the protein is exposed to solution and may be disordered. This cleavage did not produce any apparent change in the protein's specific activity or affinity for substrate.

#### Functional Characterization of HMGCLL1

To determine if HMGCLL1 is a functional HMG-CoA lyase, well characterized properties of other HMG-CoA lyases were examined for HMGCLL1. Wild-type and G2A HMGCLL1 were assayed for HMG-CoA lyase activity as described in material and methods. Wild-type and G2A HMGCLL1 specific activities were measured at 144 and 90 U/mg respectively. While the specific activity of the wild-type enzyme is comparable to that of wt recombinant human HMGCL (159 U/mg), the specific activity measured for the G2A mutant is somewhat lower due to its lower level of purity (< 95% as estimated by densitometry). Activity of HMGCLL1 is markedly stimulated by divalent cations. Wild-type and G2A HMGCLL1 exhibit  $K_m$  values for  $Mg^{2+}$  (49  $\mu$ M and 88  $\mu$ M) that are somewhat tighter than reported for recombinant human HMGCL (233  $\mu$ M) and  $K_m$  values for  $Mn^{2+}$  that are comparable (0.18, 0.24, and 0.34  $\mu$ M respectively). The  $K_m$  ( $_{(S)HMG-CoA}$ ) values measured for wt and G2A HMGCLL1 (28 and 24  $\mu$ M) are remarkably similar to those reported recombinant human HMGCL (24  $\mu$ M). A comparison of these

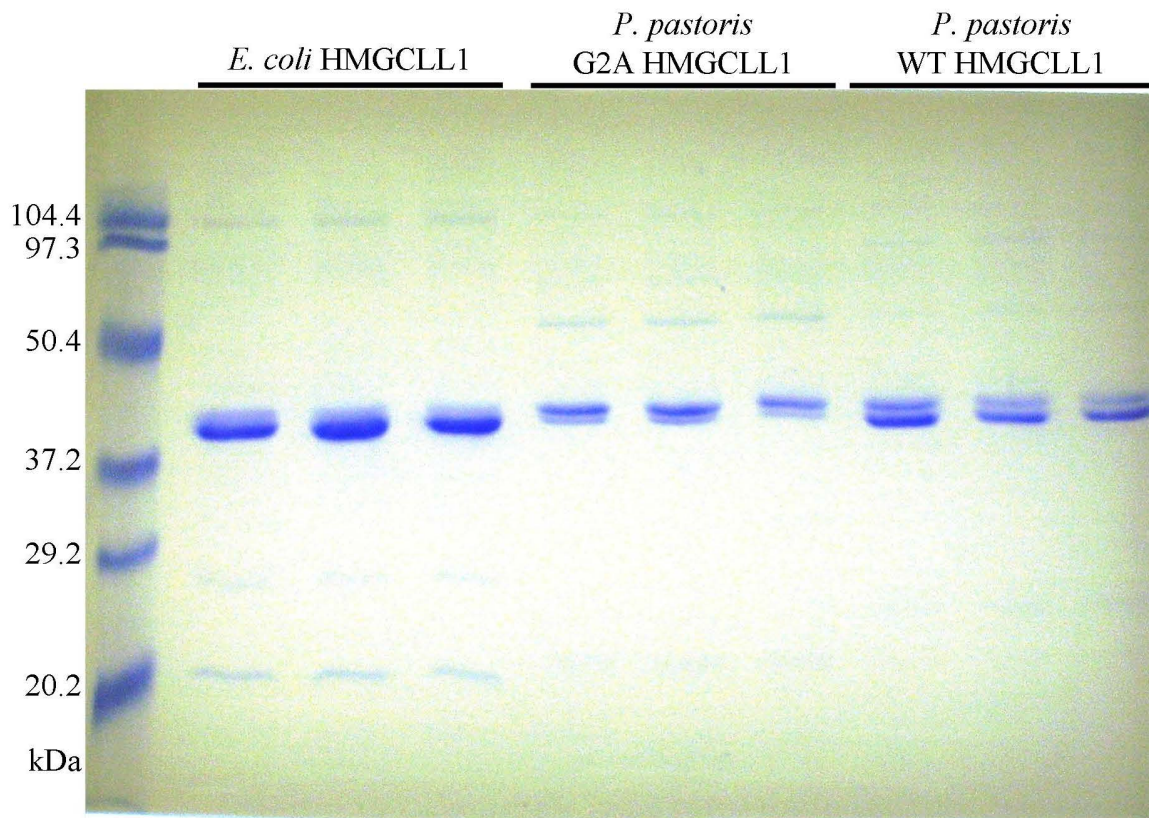


Figure 3.6. Coomassie stained Western blot of wt (lanes 1-3 and 7-9) and G2A HMGCLL1 (lanes 4-6) produced in *E. coli* (lanes 1-3) and *P. pastoris* (lanes 4-9). Wild-type HMGCLL1 produced in *E. coli* (2.4 ug/lane), G2A HMGCLL1 produced in *P. pastoris* (1.4 ug/lane) and wild-type HMGCLL1 produced in *P. pastoris* (3.2 ug/lane) were subjected to SDS-PAGE and transblotted to PVDF. Molecular weight markers include (highest to lowest): phosphorylase b, bovine serum albumin, ovalbumin, carbonic anhydrase, trypsin inhibitor, and lysozyme.

characteristics measured for HMGCLL1 and those reported for recombinant human and avian HMGCL is presented in Table 3.1. The high specific activity, along with substrate and divalent cation binding characteristics that are comparable to those of the previously characterized vertebrate HMG-CoA lyases (Table 3.1) indicate that HMGCLL1 is an authentic HMG-CoA lyase.

Table 3.1. Characterization of Human Wild-type and G2A HMGCLL1

Property	HMGCLL1		Recombinant Human HMGCL <sup>a</sup>		Avian HMGCL <sup>b</sup>
	Wild-type	G2A	Wild-type	C323S	
Specific Activity (U/mg) <sup>c,d</sup>	144 <sup>e</sup>	90 <sup>e,f</sup>	159	348	350
K <sub>m</sub> (HMG-CoA, μM) <sup>d</sup>	28 ± 3	24 ± 2	24	45	8
K <sub>m</sub> (Mg <sup>2+</sup> , μM) <sup>d</sup>	49 ± 7	88 ± 9	233	322	50
K <sub>m</sub> (Mn <sup>2+</sup> , μM) <sup>d</sup>	0.18 ± 0.06	0.24 ± 0.06	0.34	0.37	10

<sup>a</sup> Properties of human wild type and C323S HMG-CoA lyase have been described by Roberts *et al.* (1994).

<sup>b</sup> Properties of avian HMG-CoA lyase have been described by Kramer and Mizioroko (1980) and Hruz *et al.* (1992).

<sup>c</sup> Specific activities determined in the presence of 5mM DTT.

<sup>d</sup> Assays contained 3 nM wild-type or G2A HMGCLL1.

<sup>e</sup> Maximum specific activity is observed at 2.5 mM Mg<sup>++</sup>.

<sup>f</sup> Specific activity measurement utilized partially purified G2A protein.

### In-vitro Myristoylation of HMGCLL1

The N-terminal amino acids of HMGCLL1 are MGNVPS, a sequence which suggests it may substrate for N-myristoyl transferase (81). N-myristoyltransferase absolutely requires an N-terminal glycine. Mutation of the N-terminal glycine to alanine as in the G2A mutant HMGCLL1 precludes myristoylation. Low expression of HMGCLL1

protein in *P. pastoris* hindered attempts to determine if HMGCLL1 was myristoylated by endogenous *Pichia* N-myristoyltransferase. Edman degradation of wt HMGCLL1 failed to identify the native N-terminus and only the proteolytic product yielded a sequence. PTH-amino acids yields were only 20% of the expected value (Table 3.2). This may suggest that the full length protein is N-terminally modified, blocking Edman degradation. However, the native N-terminus could not be identified for the G2A mutant either and the yield was similarly low (22%). Since myristoylation is precluded in the G2A mutant, the N-termini of these proteins may be otherwise modified, perhaps by acetylation. HMGCLL1 tryptic peptides were also examined for a 210.2 Da mass shift

Table 3.2. Edman Degradation<sup>a</sup> of Wild-type and G2A HMGCLL1

Expression system	<i>E. coli</i> WT HMGCLL1		<i>Pichia</i> WT HMGCLL1		<i>Pichia</i> G2A HMGCLL1			
Expected yield	62 pmol		82 pmol		32 pmol			
	Major sequence		Minor sequence					
	Amino Acid	Yield (pmol)	Amino Acid	Yield (pmol)	Amino Acid	Yield (pmol)	Amino Acid	Yield (pmol)
	L18	42	G2	11	R19	16	R19	7
	R19	32	N3	11	E20	13	E20	9
	E20	27	V4	14	H21	8	H21	4
	H21	13	P5	10	L22	8	L22	10
	L22	30	S6	16	W23	1	W23	3
	W23	9	A7	12	I24	3	I24	7

<sup>a</sup> Edman degradation was performed by Iowa State University's Protein Core Facility

by MALDI however the N-terminal peptide could not be identified. For these reasons, an in-vitro approach was used. Denatured HMGCLL1 and G2A HMGCLL1 proteins purified from *E. coli* inclusion bodies were incubated with human N-myristoyltransferase and [<sup>3</sup>H]-myristoyl-CoA. Equal amounts of protein (densitometry estimates the intensity

of the G2A band as 72% that of the wt band; Figure 3.7B) from each reaction were run on an SDS gel and the dried gel exposed to autoradiography film. In the control reaction, HMGCLL1 incubated with [<sup>3</sup>H]-myristoyl-CoA but not N-myristoyltransferase, no signal is detected. In the wild type HMGCLL1 reaction, a signal can be seen at the expected molecular weight of 37.1 kDa indicating that HMGCLL1 is modified with [<sup>3</sup>H]-myristic acid (Figure 3.7A). In the G2A mutant reaction, no signal is seen at the expected molecular weight, confirming that this modification occurs at the N-terminal glycine.

#### Localization of HMGCLL1 in COS1 Cells

Immunofluorescence microscopy was used to determine the effect of myristoylation on the subcellular localization of HMGCLL1. HMGCLL1 protein purified from inclusion bodies was immobilized on nitrocellulose. The protein strips were then used to affinity purify the anti-HMGCLL1 antibody. Wild-type and G2A HMGCLL1 were cloned into the mammalian expression vector pcDNA3 and the proteins overexpressed in COS1 cells. Immunofluorescence microscopy reveals that the anti-HMGCLL1 antibody cross-reacts with a cytoskeletal-like protein in non-transfected COS1 cells (Figure 3.8A, left). Cells transfected with G2A mutant HMGCLL1 (Figure 3.8A, center) demonstrate a diffuse pattern which is consistent with cytoplasmic localization. However cells transfected with WT HMGCLL1 (Figure 3.8A, right) demonstrate a more punctate pattern. When cells expressing wt HMGCLL1 are treated with antibodies against HMGCLL1 and the cis-golgi marker GM130, the signals merge indicating that HMGCLL1 is localized to the golgi (Figure 3.8B). The differences in localization seen

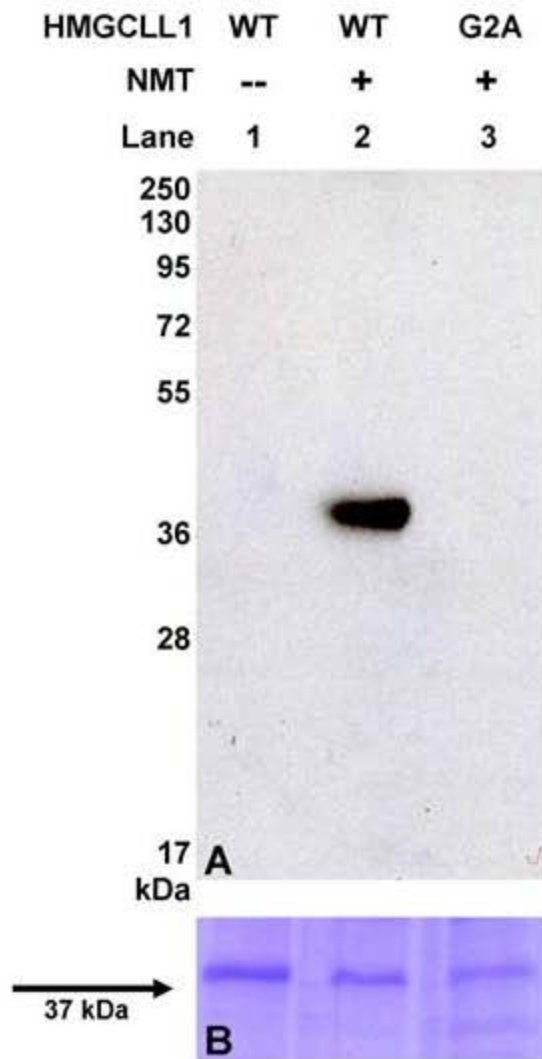
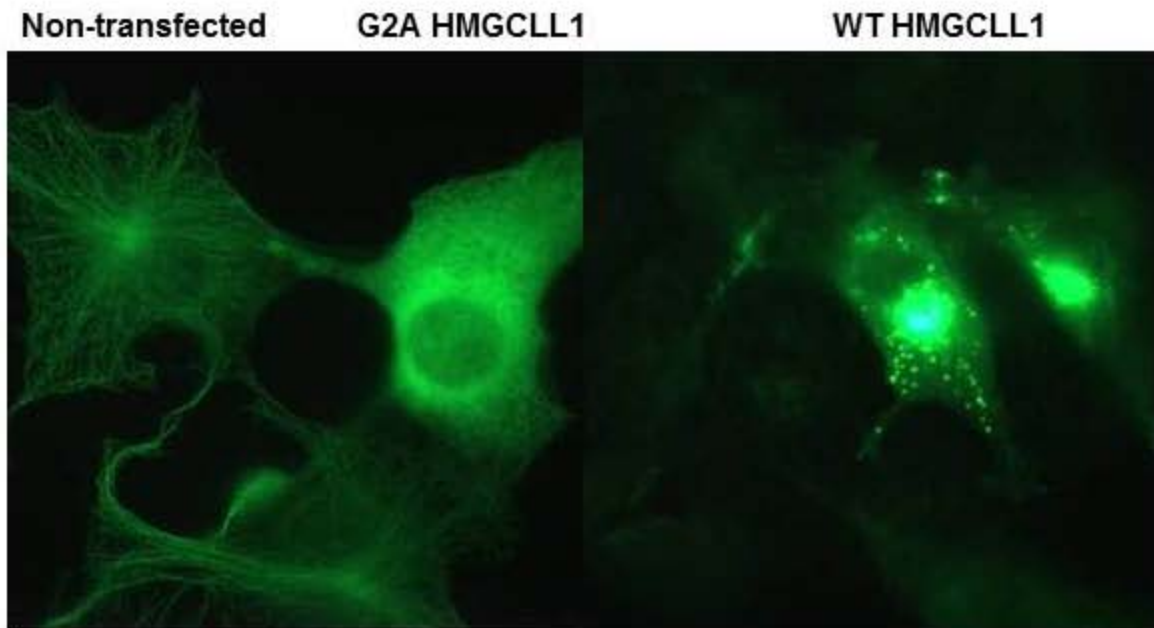
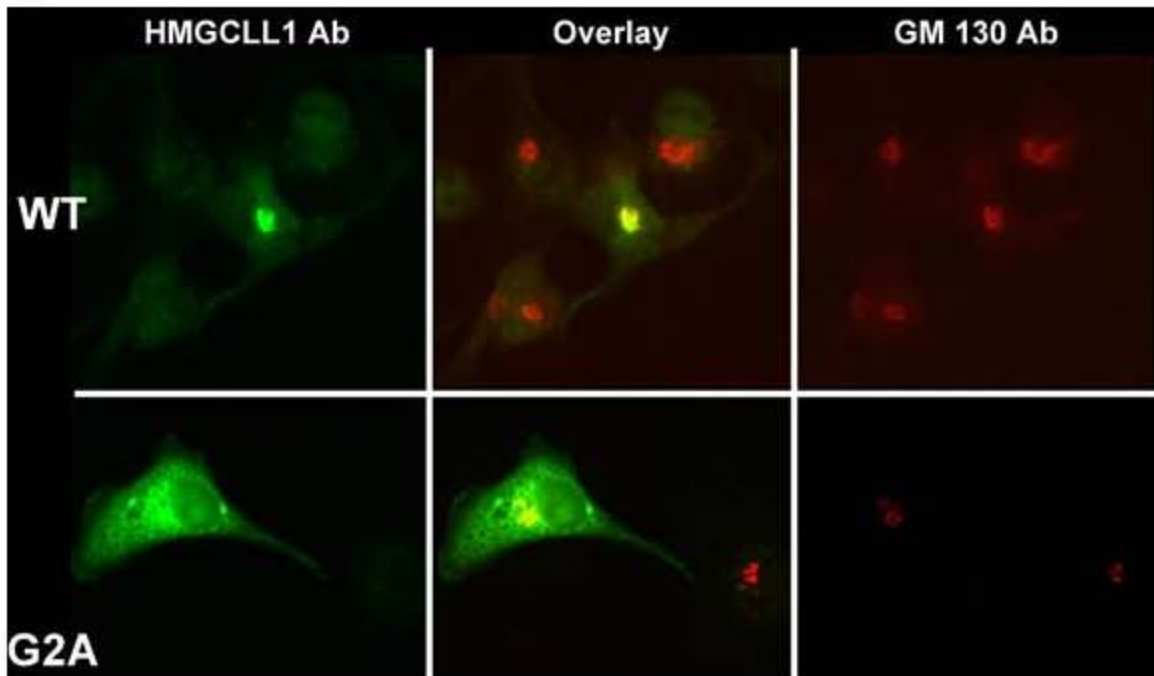


Figure 3.7. Autoradiograph demonstrating *in vitro* myristoylation of HMGCLL1 (A). Equal amounts of wild-type HMGCLL1 (lanes 1, 2, 4, 5) and G2A mutant (lane 3, 6) were incubated in separate reactions with 6.2  $\mu$ g N-myristoyltransferase (NMT) as described in materials and methods. The negative control reaction (lane 1, 4) included an equal amount of HMGCLL1 but no NMT. Protein precipitated from each reaction was run on a 12% SDS gel and the dye front was allowed to run off. The gel was dried, soaked in Fluoro-Hance, and exposed to autoradiography film for 3 days at  $-80^{\circ}\text{C}$ . Positions indicated for pre-stained molecular weight standards are determined when exposed autoradiography film is overlaid on the western blot. (B) An SDS gel run in parallel was Coomassie stained to demonstrate comparable loading of HMGCLL1 proteins.



**A**



**B**

Figure 3.8. Immunofluorescence microscopy of COS-1 cells overexpressing HMGCLL1 or G2A HMGCLL1. COS-1 cells were transfected with pcDNA3-HLL1-His6 or pcDNA3-HLL1-G2A-His6 and examined by immunofluorescence microscopy using affinity purified anti-HMGCLL1 or anti-Golgi Marker 130 primary antibodies and appropriate fluorescently labeled secondary antibodies.

upon mutation of the N-terminal glycine to an alanine suggest that myristoylation promotes the association of HMGCLL1 with subcellular membranes.

#### Endogenous Expression of HMGCLL1 in Rat Organ Lysates

Since overexpression of exogenous proteins can cause misfolding and/or aggregation, one must consider that the punctate localization of HMGCLL1 is simply an artifact. To address this issue, a cell line that endogenously expresses HMGCLL1 needed to be identified. Furthermore, the expression pattern of HMGCLL1 protein under a variety of metabolic conditions and/or during different developmental stages may be a useful tool in elucidating the physiological function of this novel HMG-CoA lyase. To screen for cell types that endogenously express HMGCLL1, an array of fed rat organ lysates was probed with anti-HMGCLL1 antibody. The 800 xg supernatant of a variety of homogenized rat organs was passed through a 0.2 micron filter prior to transfer to nitrocellulose. A duplicate array was prepared and probed with anti-avian HMGCL antibody as a control. In organ lysate blots probed with antibody against HMG-CoA lyase, strong signals can be seen in the gut (duodenum, small intestine, caecum, and large intestine) and liver (Figure 3.9A). Weaker signals can be seen in the kidney and adrenal gland. These results are consistent with current literature describing HMG-CoA lyase activity in these organs (82). In contrast, organ lysate blots probed with antibody against HMGCLL1, strong signals are seen only in the duodenum and small intestine (Figure 3.9B). In interpreting these results, it is important to keep in mind that anti-HMGCL antibody recognizes both HMGCL and HMGCLL1 (Figure 3.3B). Therefore, the signals seen in duodenum and small intestine on the anti-HMGCL blot (Figure 3.9A) may be provided primarily by

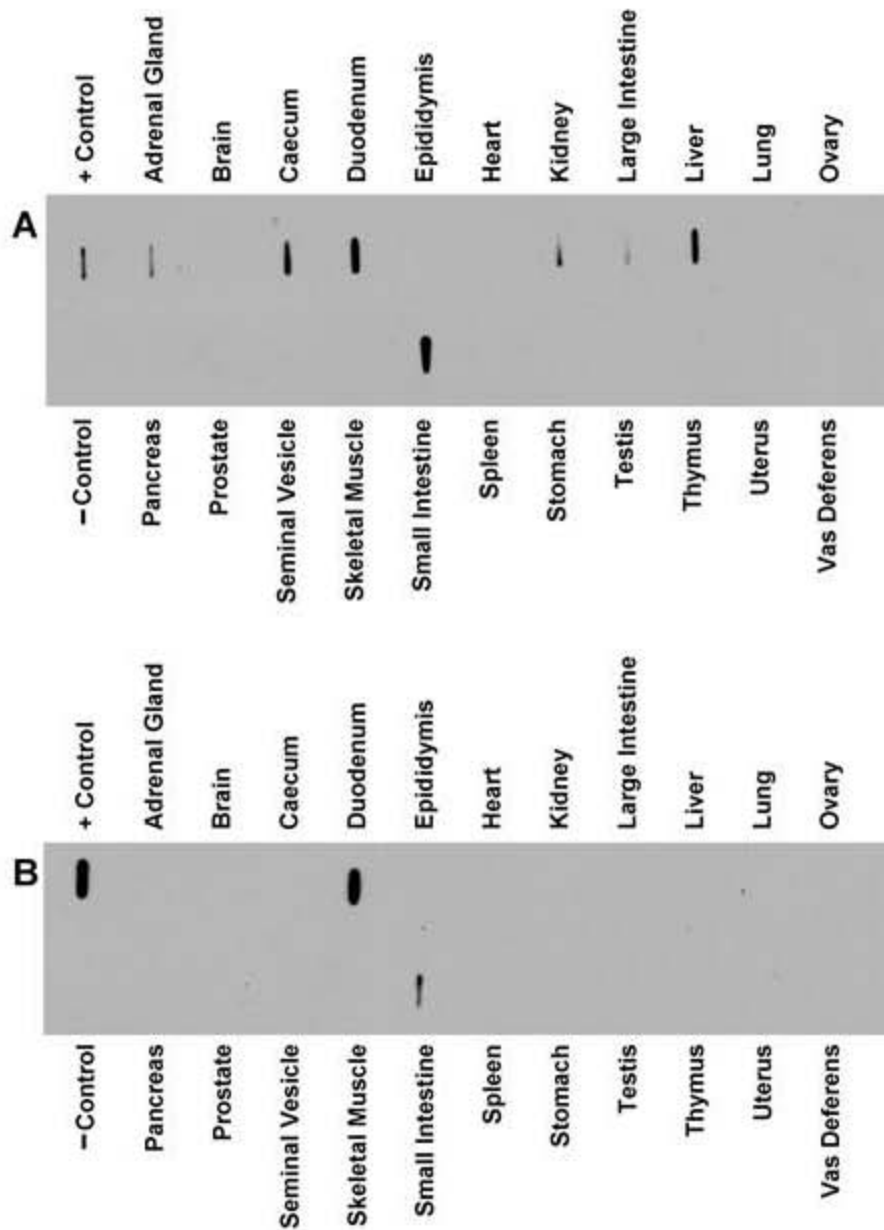


Figure 3.9. Rat organ lysate blots probed with anti-HMGCL (A) or anti-HMGCLL1 (B) antibodies. Protein (10 mg) from each clarified organ lysate was applied to nitrocellulose using a slot-blot manifold. Blocked, peroxidase suppressed blots were incubated separately with anti-HMG-CoA lyase (A) or anti-HMGCLL1 (B) antibodies. The blots were incubated with goat anti-rabbit IgG horseradish peroxidase conjugated secondary antibody and developed using enhanced chemiluminescence. The antibody against HMG-CoA lyase recognizes both mitochondrial HMG-CoA lyase and HMGCLL1 while the antibody against HMGCLL1 does not recognize mitochondrial HMG-CoA lyase (figure 3.3).

HMGCLL1 protein. Based on these results (and their availability), the human colorectal adenocarcinoma cell line Caco-2 was examined for endogenous HMGCLL1 expression. When probed with anti-HMGCLL1 antibody, blots of Caco-2 cell lysates display an immunoreactive band at the expected molecular weight (data not shown). However, the presence of multiple, intensely cross-reacting proteins preclude this cell line from being useful for subcellular localization studies. Although this experiment did not reveal a cell line useful for co-localization studies, it does demonstrate that HMGCLL1 is expressed in mammals in a pattern that is distinct from that of the traditional HMG-CoA lyase.

#### Endogenous Expression of HMGCLL1 in Human Neuroblastoma and Glioblastoma Cell Lines

Since rat organ lysate arrays failed to suggest a cell line endogenously expressing HMGCLL1 protein that would be useful for sub-cellular localization studies, the expression profile of *hmgcll1* transcripts was examined. The UniGene data base expressed sequence tag (EST) profile for *hmgcll1* reports the highest levels of transcripts in the brain (83). Thirty micrograms of protein from neuro2a (mouse neuroblastoma), SK-N-SH (human neuroblastoma), and U87 (human glioblastoma) cell lysates were subjected to SDS-PAGE and the proteins were transblotted to nitrocellulose. Thirty micrograms of protein from mouse duodenum, brain, and liver homogenates were also run as controls. As expected based on results from rat organ lysate blots (Figure 3.9B) an immunoreactive band can be seen at 37 kDa in mouse duodenum and no band is detected at 37 kDa in mouse liver (Figure 3.10). As suggested by the EST profile, a signal can also be seen at 37 kDa in mouse brain. Although no signal is apparent in samples from

the mouse neuroblastoma cell line neuro2a, very strong signals are present at 37 kDa in the human neuroblastoma cell line SK-N-SH and the human glioblastoma cell line U87. Comparison of band intensities between samples from the SK-N-SH and U87 cell lines and the mouse brain suggest that HMGCLL1 is overexpressed in these human cancer cells.

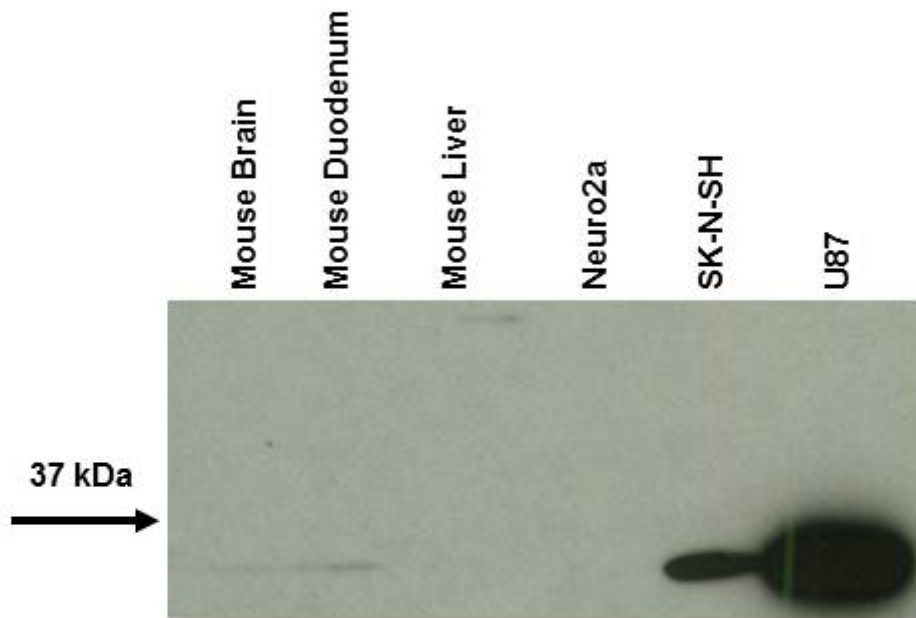


Figure 3.10. Western blot of mouse organ and human cancer cell line homogenates. Protein (30  $\mu$ g) from each homogenate was run on an SDS gel and proteins were transblotted to nitrocellulose. The blocked blot was incubated with affinity purified anti-HMGCLL1 antibody, goat anti-rabbit IgG horseradish peroxidase conjugated secondary antibody, and developed using enhanced chemiluminescence.

Since a cell line that does not overexpress HMGCLL1 was needed, the neuro2a cell line was more closely examined. Fifty micrograms of protein (instead of 30  $\mu\text{g}$  as in the previous experiment) from the high-speed supernatant of neuro2a cells was subjected to SDS-PAGE and proteins were transblotted to nitrocellulose. When probed with affinity purified anti-HMGCLL1 antibody, a light signal can be seen at the expected molecular weight of 36.3 kDa (Figure 3.11). These results suggest that the mouse neuroblastoma cell line neuro2a may be useful to identify the subcellular localization of HMGCLL1.

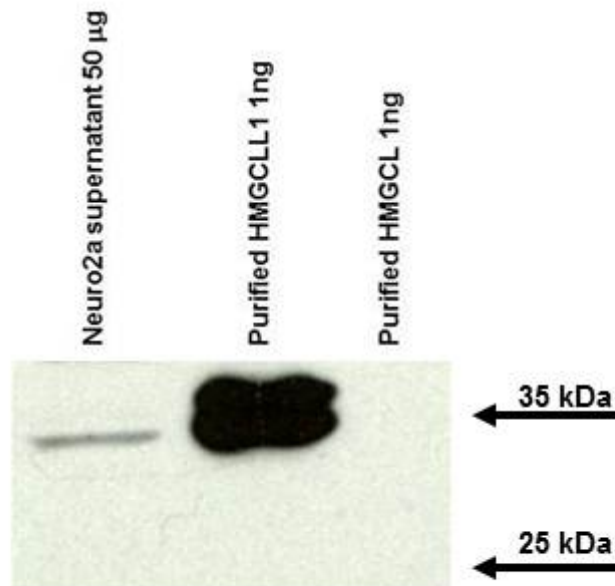


Figure 3.11. Western blot of neuro2a supernatant probed with anti-HMGCLL1 antibody. Fifty micrograms of protein from the high-speed supernatant of neuro2a cell lysate, 1 ng of purified HMGCLL1, and 1ng of purified HMGCL were run in separate lanes on an SDS gel. Proteins were transblotted to nitrocellulose and the blot probed with affinity purified anti-HMGCLL1 antibody. The blot was incubated with goat-anti rabbit IgG horseradish peroxidase conjugated secondary antibody and developed using Pierce West Pico ECL reagent. A Fermentas Page Ruler ladder was used to estimate the molecular weights.

## Indirect Immunofluorescence of HMGCLL1 in

### Neuro2a and U87 Cells

To determine the subcellular localization of HMGCLL1 in cells expressing the protein at endogenous levels, neuro2a and U87 cells were examined by immunofluorescence microscopy. Cells were grown to about 80% confluence, permeabilized, and fixed. After incubation with affinity purified anti-HMGCLL1 antibody and Alexa Fluor 488 labeled goat anti-rabbit IgG cells were examined under a fluorescent microscope fitted with the appropriate filters. The fluorescent signal observed is compact, punctate, and similar in both cell types (Figure 3.12). The expression pattern demonstrated is not consistent with a cytoplasmic, plasma membrane, endoplasmic reticulum (ER), golgi, or nuclear localization. Since HMGCLL1 is expressed at lower levels in neuro2a than in U87 cells (Figure 3.10, Figure 3.11), the neuro2a cell line was chosen for co-localization studies. Utilization of this cell line allows an endogenous subcellular localization pattern to be examined.

For co-localization studies, neuro2a cells were cultured as above. Fixed, permeabilized cells were first incubated with affinity purified rabbit anti-HMGCLL1 and a mouse or sheep antibody against a protein specific to a certain subcellular compartment. The cells were thoroughly washed and incubated with the appropriate fluorescently labeled secondary antibodies. One set of coverslips was incubated with affinity purified rabbit anti-avian HMGCL and mouse anti-ATP synthase primary antibodies as a control. When the images of a cell incubated with anti-avian HMGCL and anti-ATP synthase

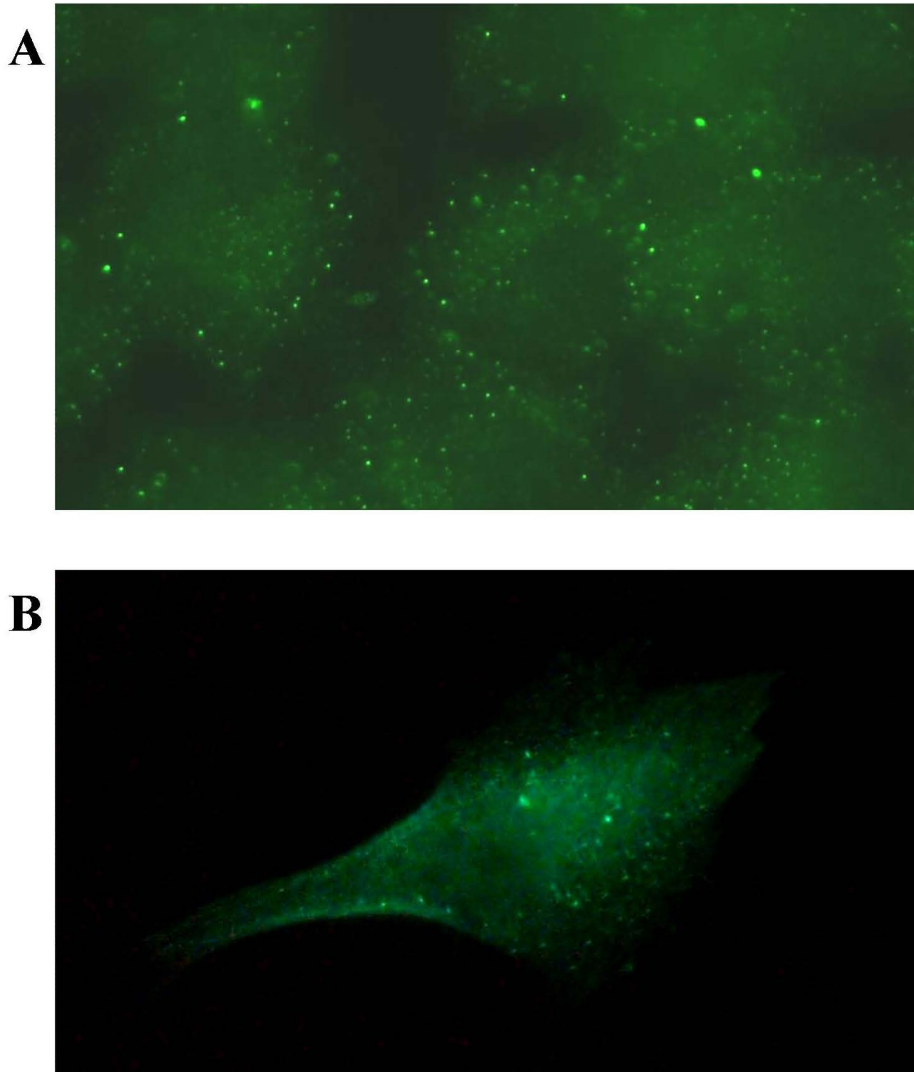


Figure 3.12. Indirect immunofluorescence of HMGCLL1 in neuro2a (A) and U87 cells (B). Neuro2a (mouse neuroblastoma) and U87 (human glioblastoma) cells were permeabilized, fixed, and incubated with affinity purified anti-HMGCLL1 antibody. Following incubation with Alexa Fluor 488 conjugated goat anti-rabbit IgG, cells were examined under a fluorescent microscope fitted with the appropriate filters.

primary antibodies are overlaid, the majority of the signal merges indicating that HMGCL is localized to the mitochondria (Figure 3.13A). Since the anti-avian HMGCL antibody also recognizes HMGCLL1, the portion of the HMGCL signal that doesn't merge with ATP synthase can be attributed to HMGCLL1. In sharp contrast, the signals do not merge in cells probed with anti-HMGCLL1 and anti-ATP synthase demonstrating that HMGCLL1 is an extramitochondrial HMG-CoA lyase (Figure 3.13B). As demonstrated in figure 3.13C, HMGCLL1 does not localize to peroxisomes as has been reported for HMGCL (84). Because of their role in cholesterol storage, lipid droplets were also examined for colocalization with HMGCLL1. Fixed, permeabilized cells were incubated with anti-HMGCLL1 and BODIPY, a fluorescent dye specific for neutral lipids (85). The fluorescent signals for HMGCLL1 and lipid droplets do not merge either, ruling lipid droplets out as the compartment to which HMGCLL1 is localized (Figure 3.13D). Although it has been shown that myristoylated HMGCLL1 localizes to a subcellular membrane which is not the plasma, nuclear, ER/Golgi, mitochondrial, peroxisomal, or lipid droplet membrane, it has yet to be determined exactly to which compartment HMGCLL1 is localized. These experiments do however demonstrate that HMGCLL1 has a subcellular localization that is distinct from that of the traditional HMG-CoA lyase.

### **Discussion**

Based on sequence homology, the National Institute of Health's Mammalian Gene Collection program identified protein encoded by the human gene *hmgcll1* as being a potential HMG-CoA lyase. Located on chromosome 6, *hmgcll1* spans 6 times more of

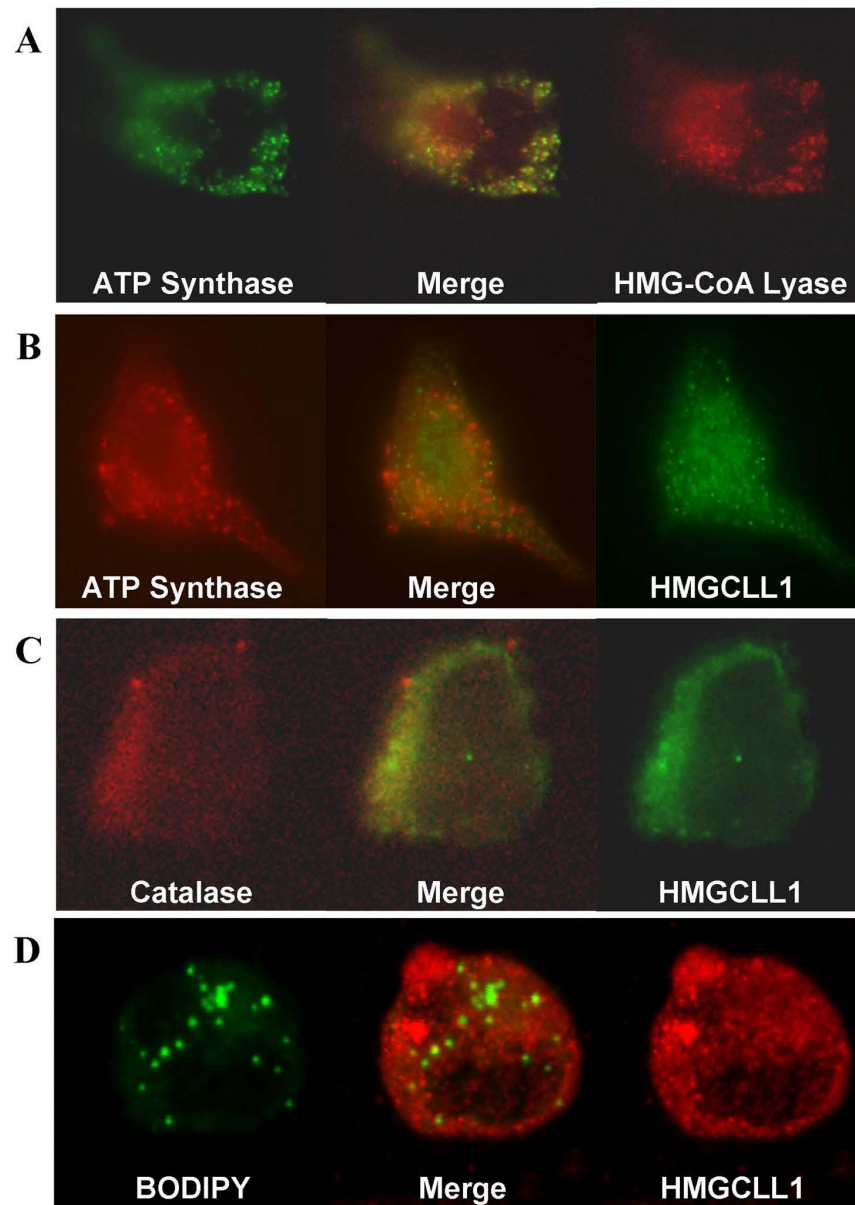


Figure 3.13. Subcellular localization of HMGCLL1 in neuro2a cells. Neuro2a cells were permeabilized, fixed, and incubated with the following primary antibodies: A) rabbit anti-avian HMGCL and mouse anti-ATP synthase (a mitochondrial marker) B) rabbit anti-HMGCLL1 and mouse anti-ATP synthase C) rabbit anti-HMGCLL1 and sheep anti-catalase (a peroxisomal marker) D) rabbit anti-HMGCLL1 and BODIPY 493/503 (stains neutral lipids) Following incubation with the appropriate fluorescently labeled secondary antibodies, cells were examined under a fluorescent microscope fitted with the appropriate filters.

the genome than does the traditional human HMG-CoA lyase, *hmgcl* does. Although the expanse of this gene suggested it may be a pseudogene, its high homology (64% identity) to HMGCL and the presence of the HMG-CoA lyase signature sequence (Figure 3.1), prompted this investigation into its functionality. The results presented here demonstrate that HMGCLL1 is indeed a functional HMG-CoA lyase with characteristics similar to those of previously characterized HMG-CoA lyases (Table 3.1). It has a specific activity, substrate binding, and metal binding characteristics similar to those of the traditional human mitochondrial HMG-CoA lyase. Despite its high homology with HMGCL, the N-terminus of the HMGCLL1 protein is unique in that it lacks a mitochondrial leader sequence and instead contains an N-myristoylation motif (Figure 3.1). This feature is conserved throughout all but one of the vertebrate HMGCLL1 genes identified to date (Figure 3.2). *In-vitro* myristoylation experiments confirm that the N-terminal amino acids of HMGCLL1 are an acceptable substrate for human N-myristoyltransferase (Figure 3.7). Indirect immunofluorescence of HMGCLL1 overexpressed in COS1 cells demonstrates a punctate localization (Figure 3.8A, right). Disruption of the N-myristoylation site by mutation of the N-terminal glycine to alanine alters the localization pattern of the protein from punctate to diffuse, which is consistent with a cytosolic localization (Figure 3.8, center). This dramatic change in localization upon disruption of the N-myristoylation site, suggests that HMGCLL1 is also myristoylated *in-vivo* and that myristoylation promotes association of the protein with a subcellular membrane. Overexpression of HMGCLL1 leads to localization of the protein in the cis-golgi (Figure 3.8B), whereas endogenous levels of expression produce protein that is localized to

cytoplasmic puncta (Figure 3.12). Endogenously expressed HMGCLL1 is not localized to mitochondria or peroxisomes (Figure 3.13) which is consistent with its lack of an N-terminal mitochondrial leader sequence or a C-terminal peroxisomal targeting motif (Figure 3.1). While the specific compartment to which HMGCLL1 is localized has not been identified, the cytoplasm, nucleus, ER/golgi, and lipid droplets have been ruled out. Although HMGCLL1 has characteristics similar to those of the mitochondrial HMG-CoA lyase, the differences in its subcellular localization and expression pattern (Figure 3.9, 3.10) suggest that it has a different physiological function.

## CHAPTER 4

### CONCLUSIONS AND FUTURE DIRECTIONS

#### **Investigation of Cysteines Mediating Intersubunit Disulfide Formation and Regulation by Thiol-Disulfide Exchange**

Although glucose is the primary fuel for the brain, the ketone bodies 3-hydroxybutyrate and acetoacetate become important for energy and/or substrate production during conditions such as fasting, starvation, and development. 3-Hydroxy-3-methylglutaryl-Coenzyme A lyase (HMG-CoA lyase) cleaves HMG-CoA into the ketone acetoacetate and acetyl-CoA, a key step in ketogenesis and the last step in leucine catabolism. HMG-CoA lyase is a homodimer containing 8 cysteines per monomer whose activity is regulated by thiol/disulfide exchange and it forms a covalent dimer upon denaturation in the absence of reductant. In this study, the contribution of each of these eight cysteines to regulation by thiol/disulfide exchange was examined and the identity of cysteines participating in intersubunit disulfide bond formation was determined. Each of the eight HMG-CoA lyase cysteines have been individually mutated to serine and the effect of the mutation on covalent dimer formation and enzyme activity in the absence of exogenous thiol examined. It was determined that the diminution of HMGCL activity upon air oxidation does not directly correlate with inter-subunit disulfide bond formation as was originally proposed. This is demonstrated by the C141S mutant which has a less than wild-type dependence on thiol for activity yet forms a strong dimer band upon non-reducing SDS-PAGE and also by the C170S mutant which has an inflated dependence on thiol for activity yet does not form a dimer band upon non-reducing SDS-PAGE. The

abolition of non-reducing SDS-PAGE dimer bands upon mutation of both C323 and C266 to serine and the restoration of non-reducing SDS-PAGE dimer bands upon co-expression of C323S and C266S to form a C266S/C323S mutant heterodimer demonstrates that C323 and C266 are the most likely partners in the inter-subunit disulfide bond that forms upon air oxidation of HMGCL. Evidence has also been presented that the C170-C174 pair competes with C323 for disulfide linkage to C266. This is demonstrated by abolition of the non-reducing SDS-PAGE dimer band upon mutation of C170 to serine and the subsequent restoration of dimer formation upon mutation of C174 to serine in a C170S background. Finally, it is suggested by this work that intra-subunit linkage between C266 and C174 participates in regulation of enzyme activity by thiol disulfide exchange. The inflated dependence on exogenous thiol for activity measured in the C170S mutant suggests that its partner (C174) is directly involved in a regulatory disulfide. This is supported by the inflated dependence on thiol measured in the C170S/C323S double mutant and by the less than wild-type dependence on thiol measured when C174 is mutated to a serine in a C170S background.

Although this work has provided experimental evidence implicating the cysteine residues directly involved in intersubunit disulfide bond formation and regulation of activity by thiol-disulfide exchange, several residues were also identified that have intermediate or indirect effects. While not on the order of the C170S mutant (640 fold), the dependence on thiol for activity displayed by the C197 and C234 mutants (150 fold and 172 fold) may warrant further investigation. While the effect of the C141S mutation on thiol dependence seems mild, it is unique among the non-catalytic cysteines in that its

mutation to serine partially relieves the enzyme of its dependence on thiol. This effect would be expected from a residue that was directly involved with C266 but did not have a favored partner of its own as with C170-C174. Construction of a series of C197S, C234S, and C141S double mutants and examination of the effect on thiol stimulation of activity and intersubunit disulfide formation may help elucidate the role these residues play in regulation of HMGCL.

### **Discovery of an Extramitochondrial Homolog of HMG-CoA Lyase**

Based on sequence homology, the National Institute of Health's Mammalian Gene Collection Program (MGC) has recently identified the protein encoded by the gene 3-hydroxymethyl-3-methylglutaryl-Coenzyme A-lyase-like 1 (HMGCLL1) as being a potential HMG-CoA lyase. Human HMG-CoA lyase is found in mitochondria and peroxisomes of many tissues (primarily in liver) however, HMGCLL1 protein lacks the mitochondrial signal peptide and transcripts are found primarily in the brain and heart. In addition, the non-conserved N-terminal region of the HMGCLL1 protein contains an N-myristoylation consensus pattern. This work describes the expression, purification, and characterization of recombinant human HMGCLL1. It was determined that HMGCLL1 has a specific activity, substrate binding, and metal binding characteristics similar to those of previously characterized HMG-CoA lyases. It has also been demonstrated that HMGCLL1 is N-terminally modified with myristic acid by human N-myristoyltransferase *in-vitro* and that this modification effects the subcellular localization of the protein *in-vivo*. Although the subcellular localization of HMGCLL1 has not yet been determined, its localization is distinct from that of HMGCL. It has been

demonstrated that HMGCLL1 is endogenously expressed in the fed rat small intestine, mouse brain, and mouse small intestine and that this expression pattern differs from that of HMGCL. Interestingly, it was also found that this protein is over-expressed in human neuroblastoma and human glioma cancer cell lines when compared to normal mouse brain.

The work reported here is an initial characterization of the HMGCLL1 protein and there are several more questions to be answered. HMGCLL1 contains 8 cysteines as does HMGCL however, it lacks the C-terminal cysteine (C323) implicated in intersubunit disulfide bond formation and instead contains an N-terminal cysteine located in its non-conserved leader sequence. In light of the work described in Chapter 2, one would expect that HMGCLL1 would not be prone to formation of a covalent dimer when denatured in the absence of reductant. However, preliminary data suggests that HMGCLL1 may also form an intersubunit disulfide. Unfortunately, low levels of expression and the susceptibility of the recombinant protein to proteolysis have hampered the investigation of this effect. The physiological role of HMGCLL1 is perhaps the most important question remaining to be answered. Is HMGCLL1 present in the cytoplasm to produce acetoacetate and/or acetyl-CoA under conditions where HMGCL is not active or is it a moonlighting protein serving as a scaffold, to regulate transcription, or some other non-enzymatic function? Determination of the subcellular localization may aid in answering this question. An examination of the expression pattern of this protein under different metabolic conditions and during different stages of development would also be useful. Finally, the impact of elevated HMGCLL1 expression in human cancer cells

should be examined. Not only could this aid in elucidation of the physiological role of HMGCLL1, but it could also identify HMGCLL1 as a potential therapeutic target.

## REFERENCE LIST

- (1) Mitchell, G. A., Kassovska-Bratinova, S., Boukaftane, Y., Robert, M. F., Wang, S. P., Ashmarina, L., Lambert, M., Lapierre, P., and Potier, E. (1995) Medical aspects of ketone body metabolism. *Clin Invest Med* 18, 193-216.
- (2) Pardridge, W. M. (1991) Blood-brain barrier transport of glucose, free fatty acids, and ketone bodies. *Adv Exp Med Biol* 291, 43-53.
- (3) Owen, O. E., Morgan, A. P., Kemp, H. G., Sullivan, J. M., Herrera, M. G., and Cahill, G. F., Jr. (1967) Brain metabolism during fasting. *J Clin Invest* 46, 1589-95.
- (4) Williamson, D. H., Bates, M. W., and Krebs, H. A. (1968) Activity and intracellular distribution of enzymes of ketone-body metabolism in rat liver. *Biochem J* 108, 353-61.
- (5) Holm, C., Osterlund, T., Laurell, H., and Contreras, J. A. (2000) Molecular mechanisms regulating hormone-sensitive lipase and lipolysis. *Annu Rev Nutr* 20, 365-93.
- (6) McGarry, J. D., and Brown, N. F. (1997) The mitochondrial carnitine palmitoyltransferase system. From concept to molecular analysis. *Eur J Biochem* 244, 1-14.
- (7) Casals, N., Roca, N., Guerrero, M., Gil-Gomez, G., Ayte, J., Ciudad, C. J., and Hegardt, F. G. (1992) Regulation of the expression of the mitochondrial 3-hydroxy-3-methylglutaryl-CoA synthase gene. Its role in the control of ketogenesis. *Biochem J* 283 (Pt 1), 261-4.
- (8) Lowe, D. M., and Tubbs, P. K. (1985) Succinylation and inactivation of 3-hydroxy-3-methylglutaryl-CoA synthase by succinyl-CoA and its possible relevance to the control of ketogenesis. *Biochem J* 232, 37-42.
- (9) Stegink, L. D., and Coon, M. J. (1968) Stereospecificity and other properties of highly purified beta-hydroxy-beta-methylglutaryl coenzyme A cleavage enzyme from bovine liver. *J Biol Chem* 243, 5272-9.
- (10) Laffel, L. (1999) Ketone bodies: a review of physiology, pathophysiology and application of monitoring to diabetes. *Diabetes Metab Res Rev* 15, 412-26.

- (11) Roberts, J. R., Narasimhan, C., Hruz, P. W., Mitchell, G. A., and Miziorko, H. M. (1994) 3-Hydroxy-3-methylglutaryl-CoA lyase: expression and isolation of the recombinant human enzyme and investigation of a mechanism for regulation of enzyme activity. *J Biol Chem* 269, 17841-6.
- (12) Chavez-Aviles, M., Diaz-Perez, A. L., Reyes-de la Cruz, H., and Campos-Garcia, J. (2009) The *Pseudomonas aeruginosa* liuE gene encodes the 3-hydroxy-3-methylglutaryl coenzyme A lyase, involved in leucine and acyclic terpene catabolism. *FEMS Microbiol Lett* 296, 117-23.
- (13) Stegink, L. D., and Coon, M. J. (1968) Stereospecificity and other properties of highly purified beta-hydroxy-beta-methylglutaryl coenzyme A cleavage enzyme from bovine liver. *J Biol Chem* 243, 5272-9.
- (14) Kramer, P. R., and Miziorko, H. M. (1980) Purification and characterization of avian liver 3-hydroxy-3-methylglutaryl coenzyme A lyase. *J Biol Chem* 255, 11023-8.
- (15) Prasanna, P., and Holmlund, C. E. (1987) Identification in *Tetrahymena pyriformis* of 3-hydroxy-3-methyl glutaryl coenzyme a lyase: its purification and properties. *Int J Biochem* 19, 385-9.
- (16) Scher, D. S., and Rodwell, V. W. (1989) 3-Hydroxy-3-methylglutaryl coenzyme A lyase from *Pseudomonas mevalonii*. *Biochim Biophys Acta* 1003, 321-6.
- (17) Fu, Z., Runquist, J. A., Forouhar, F., Hussain, M., Hunt, J. F., Miziorko, H. M., and Kim, J. J. (2006) Crystal structure of human 3-hydroxy-3-methylglutaryl-CoA Lyase: insights into catalysis and the molecular basis for hydroxymethylglutaric aciduria. *J Biol Chem* 281, 7526-32.
- (18) Forouhar, F., Hussain, M., Farid, R., Benach, J., Abashidze, M., Edstrom, W. C., Vorobiev, S. M., Xiao, R., Acton, T. B., Fu, Z., Kim, J. J., Miziorko, H. M., Montelione, G. T., and Hunt, J. F. (2006) Crystal structures of two bacterial 3-hydroxy-3-methylglutaryl-CoA lyases suggest a common catalytic mechanism among a family of TIM barrel metalloenzymes cleaving carbon-carbon bonds. *J Biol Chem* 281, 7533-45.
- (19) Wang, S., Nadeau, J. H., Duncan, A., Robert, M. F., Fontaine, G., Schappert, K., Johnson, K. R., Zietkiewicz, E., Hruz, P., Miziorko, H., and et al. (1993) 3-Hydroxy-3-methylglutaryl coenzyme A lyase (HL): cloning and characterization of a mouse liver HL cDNA and subchromosomal mapping of the human and mouse HL genes. *Mamm Genome* 4, 382-7.

- (20) Mitchell, G. A., Robert, M. F., Hruz, P. W., Wang, S., Fontaine, G., Behnke, C. E., Mende-Mueller, L. M., Schappert, K., Lee, C., Gibson, K. M., Mizioro, H. M., and et al. (1993) 3-Hydroxy-3-methylglutaryl coenzyme A lyase (HL). Cloning of human and chicken liver HL cDNAs and characterization of a mutation causing human HL deficiency. *J Biol Chem* 268, 4376-81.
- (21) Bachhawat, B. K., Robinson, W. G., and Coon, M. J. (1955) The enzymatic cleavage of beta-hydroxy-beta-methylglutaryl coenzyme A to acetoacetate and acetyl coenzyme A. *J Biol Chem* 216, 727-36.
- (22) Gould, S. J., Keller, G. A., Hosken, N., Wilkinson, J., and Subramani, S. (1989) A conserved tripeptide sorts proteins to peroxisomes. *J Cell Biol* 108, 1657-64.
- (23) Ashmarina, L. I., Rusnak, N., Mizioro, H. M., and Mitchell, G. A. (1994) 3-Hydroxy-3-methylglutaryl-CoA lyase is present in mouse and human liver peroxisomes. *J Biol Chem* 269, 31929-32.
- (24) Ribes, A., Briones, P., Vilaseca, M. A., Baraibar, R., and Gairi, J. M. (1990) Sudden death in an infant with 3-hydroxy-3-methylglutaryl-CoA lyase deficiency. *J Inherit Metab Dis* 13, 752-3.
- (25) Ozand, P. T., Devol, E. B., and Gascon, G. G. (1992) Neurometabolic diseases at a national referral center: five years experience at the King Faisal Specialist Hospital and Research Centre. *J Child Neurol* 7 Suppl, S4-11.
- (26) Gibson, K. M., Breuer, J., and Nyhan, W. L. (1988) 3-Hydroxy-3-methylglutaryl-coenzyme A lyase deficiency: review of 18 reported patients. *Eur J Pediatr* 148, 180-6.
- (27) Ribes, A., Briones, P., Vilaseca, M. A., Baraibar, R., and Gairi, J. M. (1990) Sudden death in an infant with 3-hydroxy-3-methylglutaryl-CoA lyase deficiency. *J Inherit Metab Dis* 13, 752-3.
- (28) Ozand, P. T., al Aqeel, A., Gascon, G., Brismar, J., Thomas, E., and Gleispach, H. (1991) 3-Hydroxy-3-methylglutaryl-coenzyme A (HMG-CoA) lyase deficiency in Saudi Arabia. *J Inherit Metab Dis* 14, 174-88.
- (29) Roberts, J. R., Narasimhan, C., Hruz, P. W., Mitchell, G. A., and Mizioro, H. M. (1994) 3-Hydroxy-3-methylglutaryl-CoA lyase: expression and isolation of the recombinant human enzyme and investigation of a mechanism for regulation of enzyme activity. *J Biol Chem* 269, 17841-6.

- (30) Mitchell, G. A., Robert, M. F., Hruz, P. W., Wang, S., Fontaine, G., Behnke, C. E., Mende-Mueller, L. M., Schappert, K., Lee, C., Gibson, K. M., Mizioro, H. M., and et al. (1993) 3-Hydroxy-3-methylglutaryl coenzyme A lyase (HL). Cloning of human and chicken liver HL cDNAs and characterization of a mutation causing human HL deficiency. *J Biol Chem* 268, 4376-81.
- (31) Hruz, P. W., Narasimhan, C., and Mizioro, H. M. (1992) 3-Hydroxy-3-methylglutaryl coenzyme A lyase: affinity labeling of the Pseudomonas mevalonii enzyme and assignment of cysteine-237 to the active site. *Biochemistry* 31, 6842-7.
- (32) Fu, Z., Runquist, J. A., Forouhar, F., Hussain, M., Hunt, J. F., Mizioro, H. M., and Kim, J. J. (2006) Crystal structure of human 3-hydroxy-3-methylglutaryl-CoA Lyase: insights into catalysis and the molecular basis for hydroxymethylglutaric aciduria. *J Biol Chem* 281, 7526-32.
- (33) Fu, Z., Runquist, J. A., Montgomery, C., Mizioro, H. M., and Kim, J. J. Functional insights into human HMG-CoA lyase from structures of Acyl-CoA-containing ternary complexes. *J Biol Chem* 285, 26341-9.
- (34) Melov, S., Coskun, P., Patel, M., Tuinstra, R., Cottrell, B., Jun, A. S., Zastawny, T. H., Dizdaroglu, M., Goodman, S. I., Huang, T. T., Mizioro, H., Epstein, C. J., and Wallace, D. C. (1999) Mitochondrial disease in superoxide dismutase 2 mutant mice. *Proc Natl Acad Sci U S A* 96, 846-51.
- (35) Kramer, P. R., and Mizioro, H. M. (1980) Purification and characterization of avian liver 3-hydroxy-3-methylglutaryl coenzyme A lyase. *J Biol Chem* 255, 11023-8.
- (36) Hruz, P. W., and Mizioro, H. M. (1992) Avian 3-hydroxy-3-methylglutaryl-CoA lyase: sensitivity of enzyme activity to thiol/disulfide exchange and identification of proximal reactive cysteines. *Protein Sci* 1, 1144-53.
- (37) Roberts, J. R., Narasimhan, C., Hruz, P. W., Mitchell, G. A., and Mizioro, H. M. (1994) 3-Hydroxy-3-methylglutaryl-CoA lyase: expression and isolation of the recombinant human enzyme and investigation of a mechanism for regulation of enzyme activity. *J Biol Chem* 269, 17841-6.
- (38) Fu, Z., Runquist, J. A., Forouhar, F., Hussain, M., Hunt, J. F., Mizioro, H. M., and Kim, J. J. (2006) Crystal structure of human 3-hydroxy-3-methylglutaryl-CoA Lyase: insights into catalysis and the molecular basis for hydroxymethylglutaric aciduria. *J Biol Chem* 281, 7526-32.

- (39) Hruz, P. W., and Miziorko, H. M. (1992) Avian 3-hydroxy-3-methylglutaryl-CoA lyase: sensitivity of enzyme activity to thiol/disulfide exchange and identification of proximal reactive cysteines. *Protein Sci* 1, 1144-53.
- (40) Roberts, J. R., Narasimhan, C., Hruz, P. W., Mitchell, G. A., and Miziorko, H. M. (1994) 3-Hydroxy-3-methylglutaryl-CoA lyase: expression and isolation of the recombinant human enzyme and investigation of a mechanism for regulation of enzyme activity. *J Biol Chem* 269, 17841-6.
- (41) Roberts, J. R., Narasimhan, C., Hruz, P. W., Mitchell, G. A., and Miziorko, H. M. (1994) 3-Hydroxy-3-methylglutaryl-CoA lyase: expression and isolation of the recombinant human enzyme and investigation of a mechanism for regulation of enzyme activity. *J Biol Chem* 269, 17841-6.
- (42) Bradford, M. M. (1976) A rapid and sensitive method for the quantitation of microgram quantities of protein utilizing the principle of protein-dye binding. *Anal Biochem* 72, 248-54.
- (43) Stegink, L. D., and Coon, M. J. (1968) Stereospecificity and other properties of highly purified beta-hydroxy-beta-methylglutaryl coenzyme A cleavage enzyme from bovine liver. *J Biol Chem* 243, 5272-9.
- (44) Kramer, P. R., and Miziorko, H. M. (1980) Purification and characterization of avian liver 3-hydroxy-3-methylglutaryl coenzyme A lyase. *J Biol Chem* 255, 11023-8.
- (45) Goldfarb, S., and Pitot, H. C. (1971) Improved assay of 3-hydroxy-3-methylglutaryl coenzyme A reductase. *J Lipid Res* 12, 512-5.
- (46) Laemmli, U. K. (1970) Cleavage of structural proteins during the assembly of the head of bacteriophage T4. *Nature* 227, 680-5.
- (47) Fu, Z., Runquist, J. A., Forouhar, F., Hussain, M., Hunt, J. F., Miziorko, H. M., and Kim, J. J. (2006) Crystal structure of human 3-hydroxy-3-methylglutaryl-CoA Lyase: insights into catalysis and the molecular basis for hydroxymethylglutaric aciduria. *J Biol Chem* 281, 7526-32.
- (48) DeLano, W. (2002) The PyMOL Molecular Graphics System. <http://www.pymol.org>.

- (49) Fu, Z., Runquist, J. A., Forouhar, F., Hussain, M., Hunt, J. F., Mizioro, H. M., and Kim, J. J. (2006) Crystal structure of human 3-hydroxy-3-methylglutaryl-CoA Lyase: insights into catalysis and the molecular basis for hydroxymethylglutaric aciduria. *J Biol Chem* 281, 7526-32.
- (50) Guex, N., and Peitsch, M. C. (1997) SWISS-MODEL and the Swiss-PdbViewer: an environment for comparative protein modeling. *Electrophoresis* 18, 2714-23.
- (51) Kramer, P. R., and Mizioro, H. M. (1980) Purification and characterization of avian liver 3-hydroxy-3-methylglutaryl coenzyme A lyase. *J Biol Chem* 255, 11023-8.
- (52) Roberts, J. R., Narasimhan, C., Hruz, P. W., Mitchell, G. A., and Mizioro, H. M. (1994) 3-Hydroxy-3-methylglutaryl-CoA lyase: expression and isolation of the recombinant human enzyme and investigation of a mechanism for regulation of enzyme activity. *J Biol Chem* 269, 17841-6.
- (53) Roberts, J. R., Narasimhan, C., Hruz, P. W., Mitchell, G. A., and Mizioro, H. M. (1994) 3-Hydroxy-3-methylglutaryl-CoA lyase: expression and isolation of the recombinant human enzyme and investigation of a mechanism for regulation of enzyme activity. *J Biol Chem* 269, 17841-6.
- (54) Hruz, P. W., Narasimhan, C., and Mizioro, H. M. (1992) 3-Hydroxy-3-methylglutaryl coenzyme A lyase: affinity labeling of the *Pseudomonas mevalonii* enzyme and assignment of cysteine-237 to the active site. *Biochemistry* 31, 6842-7.
- (55) Roberts, J. R., Narasimhan, C., and Mizioro, H. M. (1995) Evaluation of cysteine 266 of human 3-hydroxy-3-methylglutaryl-CoA lyase as a catalytic residue. *J Biol Chem* 270, 17311-6.
- (56) Roberts, J. R., Narasimhan, C., Hruz, P. W., Mitchell, G. A., and Mizioro, H. M. (1994) 3-Hydroxy-3-methylglutaryl-CoA lyase: expression and isolation of the recombinant human enzyme and investigation of a mechanism for regulation of enzyme activity. *J Biol Chem* 269, 17841-6.
- (57) Fu, Z., Runquist, J. A., Forouhar, F., Hussain, M., Hunt, J. F., Mizioro, H. M., and Kim, J. J. (2006) Crystal structure of human 3-hydroxy-3-methylglutaryl-CoA Lyase: insights into catalysis and the molecular basis for hydroxymethylglutaric aciduria. *J Biol Chem* 281, 7526-32.
- (58) Roberts, J. R., Narasimhan, C., and Mizioro, H. M. (1995) Evaluation of cysteine 266 of human 3-hydroxy-3-methylglutaryl-CoA lyase as a catalytic residue. *J Biol Chem* 270, 17311-6.

- (59) Chivers, P. T., Laboissiere, M. C., and Raines, R. T. (1996) The CXXC motif: imperatives for the formation of native disulfide bonds in the cell. *Embo J* 15, 2659-67.
- (60) Fu, Z., Runquist, J. A., Forouhar, F., Hussain, M., Hunt, J. F., Mizioro, H. M., and Kim, J. J. (2006) Crystal structure of human 3-hydroxy-3-methylglutaryl-CoA Lyase: insights into catalysis and the molecular basis for hydroxymethylglutaric aciduria. *J Biol Chem* 281, 7526-32.
- (61) Anderson, D. H., and Rodwell, V. W. (1989) Nucleotide sequence and expression in Escherichia coli of the 3-hydroxy-3-methylglutaryl coenzyme A lyase gene of Pseudomonas mevalonii. *J Bacteriol* 171, 6468-72.
- (62) Hruz, P. W., and Mizioro, H. M. (1992) Avian 3-hydroxy-3-methylglutaryl-CoA lyase: sensitivity of enzyme activity to thiol/disulfide exchange and identification of proximal reactive cysteines. *Protein Sci* 1, 1144-53.
- (63) Fu, Z., Runquist, J. A., Forouhar, F., Hussain, M., Hunt, J. F., Mizioro, H. M., and Kim, J. J. (2006) Crystal structure of human 3-hydroxy-3-methylglutaryl-CoA Lyase: insights into catalysis and the molecular basis for hydroxymethylglutaric aciduria. *J Biol Chem* 281, 7526-32.
- (64) Guzman, M. and C. Blazquez (2004). "Ketone body synthesis in the brain: possible neuroprotective effects." *Prostaglandins Leukot Essent Fatty Acids* 70(3): 287-92.
- (65) Kashiwaya, Y., T. Takeshima, et al. (2000). "D-beta-hydroxybutyrate protects neurons in models of Alzheimer's and Parkinson's disease." *Proc Natl Acad Sci U S A* 97(10): 5440-4.
- (66) Gerhard, D. S., L. Wagner, et al. (2004). "The status, quality, and expansion of the NIH full-length cDNA project: the Mammalian Gene Collection (MGC)." *Genome Res* 14(10B): 2121-7.
- (67) Lennon, G., Auffray, C., Polymeropoulos, M., and Soares, M. B. (1996) The I.M.A.G.E. Consortium: an integrated molecular analysis of genomes and their expression. *Genomics* 33, 151-2.
- (68) Romanos, M. A., Scorer, C. A., and Clare, J. J. (1992) Foreign gene expression in yeast: a review. *Yeast* 8, 423-88.
- (69) Bradford, M. M. (1976) A rapid and sensitive method for the quantitation of microgram quantities of protein utilizing the principle of protein-dye binding. *Anal Biochem* 72, 248-54.

- (70) Pringle, J. R., Preston, R. A., Adams, A. E., Stearns, T., Drubin, D. G., Haarer, B. K., and Jones, E. W. (1989) Fluorescence microscopy methods for yeast. *Methods Cell Biol* 31, 357-435.
- (71) Linder, S., Schliwa, M., and Kube-Grandenath, E. (1996) Direct PCR screening of *Pichia pastoris* clones. *Biotechniques* 20, 980-2.
- (72) Bradford, M. M. (1976) A rapid and sensitive method for the quantitation of microgram quantities of protein utilizing the principle of protein-dye binding. *Anal Biochem* 72, 248-54.
- (73) Stegink, L. D., and Coon, M. J. (1968) Stereospecificity and other properties of highly purified beta-hydroxy-beta-methylglutaryl coenzyme A cleavage enzyme from bovine liver. *J Biol Chem* 243, 5272-9.
- (74) Kramer, P. R., and Mizioroko, H. M. (1980) Purification and characterization of avian liver 3-hydroxy-3-methylglutaryl coenzyme A lyase. *J Biol Chem* 255, 11023-8.
- (75) Goldfarb, S., and Pitot, H. C. (1971) Improved assay of 3-hydroxy-3-methylglutaryl coenzyme A reductase. *J Lipid Res* 12, 512-5.
- (76) Bradford, M. M. (1976) A rapid and sensitive method for the quantitation of microgram quantities of protein utilizing the principle of protein-dye binding. *Anal Biochem* 72, 248-54.
- (77) Towler, D. A., Adams, S. P., Eubanks, S. R., Towery, D. S., Jackson-Machelski, E., Glaser, L., and Gordon, J. I. (1988) Myristoyl CoA:protein N-myristoyltransferase activities from rat liver and yeast possess overlapping yet distinct peptide substrate specificities. *J Biol Chem* 263, 1784-90.
- (78) Hruz, P. W., and Mizioroko, H. M. (1992) Avian 3-hydroxy-3-methylglutaryl-CoA lyase: sensitivity of enzyme activity to thiol/disulfide exchange and identification of proximal reactive cysteines. *Protein Sci* 1, 1144-53.
- (79) Roberts, J. R., Narasimhan, C., Hruz, P. W., Mitchell, G. A., and Mizioroko, H. M. (1994) 3-Hydroxy-3-methylglutaryl-CoA lyase: expression and isolation of the recombinant human enzyme and investigation of a mechanism for regulation of enzyme activity. *J Biol Chem* 269, 17841-6.

- (80) Montgomery, C., and Miziorko, H. M. Influence of multiple cysteines on human 3-hydroxy-3-methylglutaryl-CoA lyase activity and formation of inter-subunit adducts. *Arch Biochem Biophys* 511, 48-55.
- (81) Towler, D. A., Adams, S. P., Eubanks, S. R., Towery, D. S., Jackson-Machelski, E., Glaser, L., and Gordon, J. I. (1988) Myristoyl CoA:protein N-myristoyltransferase activities from rat liver and yeast possess overlapping yet distinct peptide substrate specificities. *J Biol Chem* 263, 1784-90.
- (82) Bachhawat, B. K., Robinson, W. G., and Coon, M. J. (1955) The enzymatic cleavage of beta-hydroxy-beta-methylglutaryl coenzyme A to acetoacetate and acetyl coenzyme A. *J Biol Chem* 216, 727-36.
- (83) <http://www.ncbi.nlm.nih.gov/UniGene/ESTProfileViewer.cgi?uglist=Hs.147054>
- (84) Ashmarina, L. I., Rusnak, N., Miziorko, H. M., and Mitchell, G. A. (1994) 3-Hydroxy-3-methylglutaryl-CoA lyase is present in mouse and human liver peroxisomes. *J Biol Chem* 269, 31929-32.
- (85) Gocze, P. M., and Freeman, D. A. (1994) Factors underlying the variability of lipid droplet fluorescence in MA-10 Leydig tumor cells. *Cytometry* 17, 151-8.

## VITA

Christa Lynn Cochran Montgomery was born on June 3, 1972 in Kansas City, Missouri. She was educated in local public schools and graduated from Kearney High School in 1990. Christa continued her education at Maple Woods Community College followed by the University of Missouri at Kansas City from which she graduated in 1995 with a major in biology and a minor in chemistry. After taking several years off to raise her children, Christa returned to the University of Missouri at Kansas City to attend graduate school in 2004. Christa was awarded a Master's of Science degree in Molecular Biology and Biochemistry in 2007. Christa successfully defended her dissertation in November 2011. Her dissertation work resulted in one first author and one middle author publication.